

# Rock Magnetic and Petrographical–Mineralogical Studies of the Dredged Rocks from the Submarine Volcanoes of the Sea-of-Okhotsk Slope within the Northern Part of the Kuril Island Arc

V. A. Rashidov<sup>a</sup>, O. V. Pilipenko<sup>b</sup>, and V. V. Petrova<sup>c</sup>

<sup>a</sup> *Institute of Volcanology and Seismology, Russian Academy of Sciences,  
bulv. Piip 9, 683006 Petropavlovsk-Kamchatskii, Russia*

*e-mail: rashidva@kscnet.ru*

<sup>b</sup> *Schmidt Institute of Physics of the Earth, Russian Academy of Sciences,  
ul. B. Gruzinskaya 10, Moscow, 123995 Russia*

*e-mail: pilipenko@ifz.ru*

<sup>c</sup> *Geological Institute, Russian Academy of Sciences, Pyzhevskii per. 7, Moscow, 119017 Russia*

*e-mail: v.petrova.v@gmail.com*

Received March 1, 2015; in final form, May 28, 2015

**Abstract**—The rock magnetic properties of the samples of dredged rocks composing the submarine volcanic edifices within the Sea-of-Okhotsk slope of the northern part of the Kuril Island Arc are studied. The measurements of the standard rock magnetic parameters, thermomagnetic analysis, petrographical studies, and microprobe investigations have been carried out. The magnetization of the studied rocks is mainly carried by the pseudo-single domain and multidomain titanomagnetite and low-Ti titanomagnetite grains. The high values of the natural remanent magnetization are due to the pseudo-single-domain structure of the titanomagnetite grains, whereas the high values of magnetic susceptibility are associated with the high concentration of ferrimagnetic grains. The highest Curie points are observed in the titanomagnetite grains of the igneous rocks composing the edifices of the Smirnov, Edelshtein, and 1.4 submarine volcanoes.

**Keywords:** Kuril Island Arc, Sea-of-Okhotsk slope, submarine volcanoes, rock magnetic properties, titanomagnetite

**DOI:** 10.1134/S1069351316040066

## INTRODUCTION

Comprehensive exploration of the World Ocean ranks among the top-priority present day challenges of modern science. An important focus of the multidisciplinary research in this field is associated with the geological sciences.

The joint interpretation of the geological and geophysical data obtained in the expeditions of the oceanographic research vessels (ORVs) in the World Ocean provided the data about the geological structure of the regions covered by the ocean, distribution of minerals across the oceanic floor, geodynamics of the lithosphere, and relationship between volcanism and mantle sources. A close correlation is revealed between the magnetic anomalies and magnetic properties of the rocks composing different structures in the World Ocean.

It has been established that the magnetism of igneous rocks primarily depends on titanomagnetites of various compositions and degree of oxidation. This

finding was greatly promoted by the rock magnetic studies conducted by the Soviet and Russian geophysicists (Didenko, 1989; Didenko and Tikhonov, 1991; Didenko et al., 1999; Kurochkina, 2007; *Magnitnoe ...*, 1993; Pecherskii et al., 1979; 1980; 1981; Popov et al., 1989; 2011; Popov and Shcherbakov, 2001; *Priroda ...*, 1996; Shreider et al., 1982; Trukhin et al., 2000; 2001; 2005; 2006; Verba et al., 2000).

An important contribution to studying the Pacific transition zone whose western part accommodates a large cluster of submarine volcanoes was provided by the combined geological-geophysical studies aboard the *Vulkanolog* ORV in 1977–1991 (Anikieva et al., 2008; Babayants et al., 2005; 2006; Blokh et al., 2006a; 2012a; 2012b; 2013a; 2014a; Bondarenko et al., 1994; Brusilovskii et al., 2004; *Podvodnyi ...*, 1992; Rashidov, 2010; Rashidov et al., 2014; 2015; etc.).

The investigation of both active and dormant submarine volcanoes, as well as paleovolcanoes, is a topical task of utmost importance. From the standpoint of

the fundamental problems of geotectonics and geodynamics, the submarine volcanoes are efficient proxies for the geodynamical processes forming the lithosphere of the World Ocean. At the same time, exploration of the submarine volcanoes is also vital for practical applications since the processes ongoing in the present-day active volcanic regions cause a huge direct impact on the environment and human life.

From the very beginning, ever since the pioneering studies of the anomalous magnetic field of the submarine volcanoes and seamounts, research has been conducted in two mutually complementary directions covering the analysis of the paleomagnetic characteristics and identification of the geological structure and evolution of these objects. The research largely involves mathematical modeling and investigation of the magnetization of the rocks composing the volcanic edifices.

In the paleomagnetic studies of the submarine volcanoes, based on the joint analysis of the echo soundings and marine magnetic survey data, the magnitude and orientation of the effective magnetization vector are calculated by the seamount method (*Plate ...*, 1973), after which the coordinates of the virtual paleomagnetic poles are determined. These estimates allow determining the formation time of the volcanic edifices and, if the absolute age of the rocks is known, conducting the geodynamic reconstructions. One of the key limitations of the seamount method lies in the assumption that the magnetization of the seamount is represented by the remanent component alone.

In the structural geological studies, the structure of the submarine volcanoes and their evolution are studied based on the magnetic field simulations and laboratory determinations of the magnetic properties of the dredged rocks.

The data about the magnetic properties of the rocks dredged from the edifices of the submarine volcanoes are necessary for interpreting the combined geological-geophysical studies, in particular, for identifying the nature of the magnetic anomalies above the submarine volcanoes and exploring the acquisition of magnetization by the rocks during the evolution of the volcanic structures. The empirical magnetization estimates mitigate the ambiguity of the solution of the inverse problem of magnetic prospecting.

To date, the rock magnetic studies of the material from the submarine volcanic edifices in the western part of the Pacific have been carried out for the active Axial submarine volcano within the Juan de Fuca Range (*Magnitnoe ...*, 1993), Emperor Seamounts (Carvallo et al., 2004), Izu-Bonin serpentine seamounts (Stokking et al., 1992), submarine slopes of the Hawaiian Mauna Loa and Mauna Kea volcanoes (Kontny et al., 2003), and the seamount beneath the Central and Southern highs of the Shatskii Rise (Popov and Shcherbakov, 2001).

In the past few years, we have conducted the rock magnetic and petrographical-mineralogical studies of the rocks dredged from the edifices of the Late Cenozoic submarine volcanoes during the expeditions of the Vulkanolog ORV in the western part of the Pacific (Blokh et al., 2014a; Pilipenko and Rashidov, 2013; Pilipenko et al., 2012a; 2012b; 2014a; 2014b; Rashidov et al., 2012; 2014; 2015). As a result of these works, a series of active submarine volcanoes have been studied: the Fukujin and Esmeralda Bank volcanoes within the Mariana Island Arc, the Kovachi and Simbo within the Solomon Island Arc, the Ile des Cendres in the South China Sea, and the Sofu submarine volcanic cluster in the Izu-Bonin Island Arc (Rashidov et al., 2014; 2015).

Our present studies are focused on the Late Cenozoic submarine volcanoes on the Sea-of-Okhotsk slope of the Kuril Island Arc (KIA) (Pilipenko et al., 2014a; 2014b), whose rock magnetic properties have been quite poorly explored to date. The studies with such a high degree of detail are conducted for this region for the first time.

The previous measurements of the natural remanent magnetization (NRM) and magnetic susceptibility ( $k$ ) of the rocks dredged during the cruises of the Vulkanolog ORV from the edifices of the submarine volcanoes of KIA were carried out by the MA-21 astatic magnetometer (designed by Geologorazvedka, Soviet Union) at the Institute of Volcanology and Seismology of the Russian Academy of Sciences (IVS RAS). These measurements revealed a strong differentiation of these rocks by their characteristics, with the fresh unaltered varieties being most magnetic (Blokh et al., 2006a; 2012a; 2012b; 2014a; 2013b; 2014b; *Podvodnyi ...*, 1992; Rashidov, 2010; Rashidov and Bondarenko, 1998; 2003; 2004; [http://www.kscnet.ru/ivs/grant/grant\\_04/tables/magnit.xls](http://www.kscnet.ru/ivs/grant/grant_04/tables/magnit.xls)). These results fairly well agree with the data for the magnetic properties of the rocks measured within KIA. For instance, the measurements of  $k$  in the Kuril part of the Sea of Okhotsk by the Sakhalin geophysicists have demonstrated a broad scatter of the obtained values (*Geologo-geofizicheskii ...*, 1987; Korenev, 1990; Korenev et al., 1982; Korenev and Shkut', 1979; Kochergin et al., 1980), whereas the studies of the gabbroid inclusions in the young lavas of the Kuril islands, which were conducted by the researchers of the Schmidt Institute of Physics of the Earth of the Russian Academy of Sciences (IPE RAS), revealed a significant variation in  $k$  and the Koenigsberger ratio ( $Q_n$ ) (Ermakov and Pecherskii, 1989).

In this work, we present the results of the rock magnetic and petrographical-mineralogical studies of the rocks dragged from five submarine KIA volcanoes (Fig. 1) (namely, the Grigor'ev, 1.4, Smirnov, Belyankin, and Edelshtein volcanoes) which were explored in several cruises of the Vulkanolog ORV (Babayants et al., 2005; 2006; Blokh et al., 2006a; 2006b; Bondarenko et al., 1994; *Podvodnyi ...*, 1992; Rashidov, 2010;

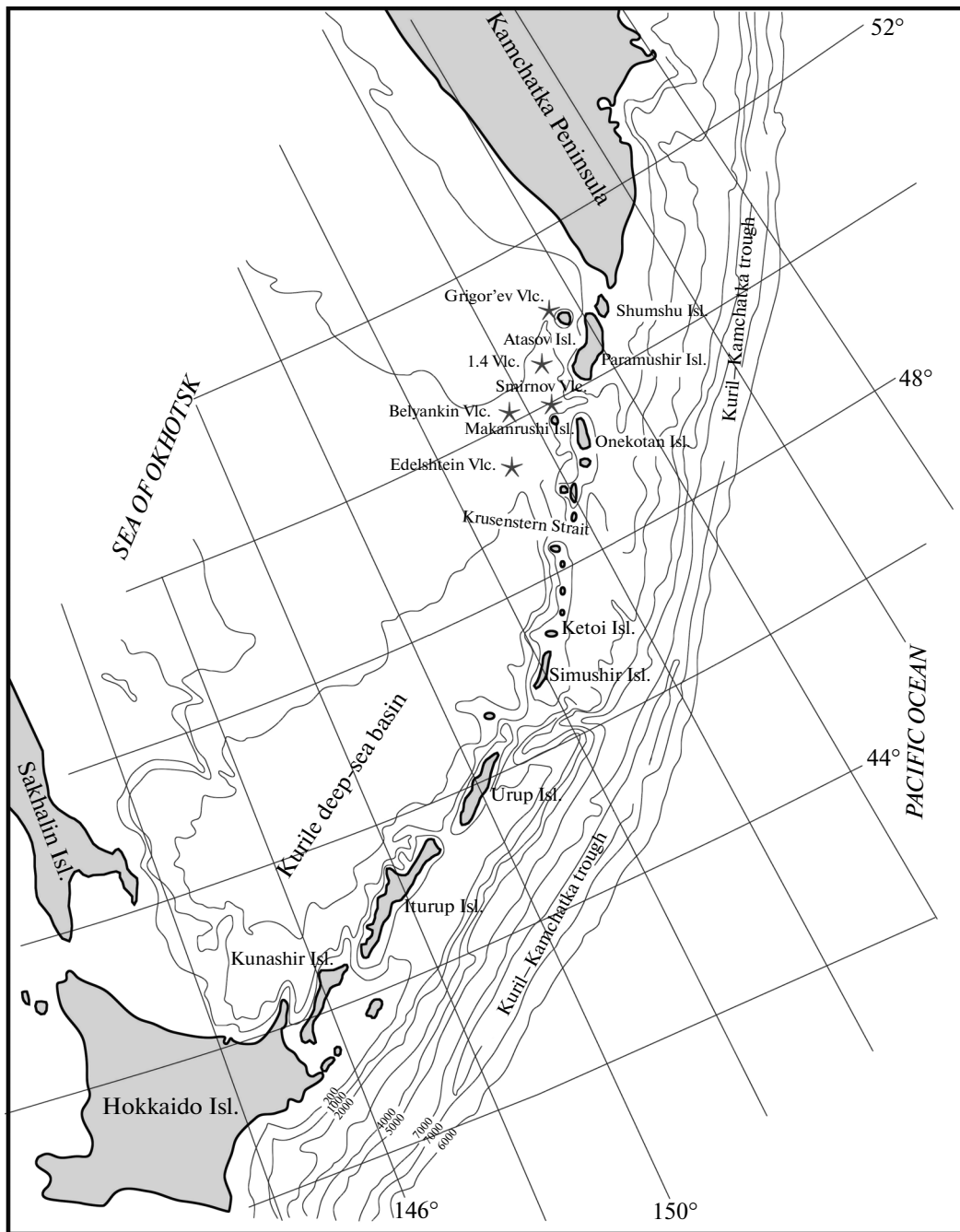


Fig. 1. The layout of the studied submarine volcanoes of the Sea of Okhotsk shelf in the northern part of KIA.

Rashidov and Bondarenko, 1998; 2003; Rashidov et al., 1992).

The purpose of the work is to study the structural features, concentration and composition of the titanomagnetites contained in the rocks composing the studied volcanoes for identifying the distinctions in the magnetic properties of these rocks and exploring the contributions of the remanent and induced magnetization in the observed anomalies of the magnetic field.

## METHODS OF STUDY

The rock magnetic studies were carried out at Schmidt Institute of Physics of the Earth of the Russian Academy of Sciences. The NRM was measured by the JR-6 magnetometer (Czech Republic); magnetic susceptibility  $k$  and  $P'$ —AGICO the degrees of anisotropy of magnetic susceptibility (AMS)—were estimated by the Multi-Function Kappabridge (AGICO, Czech Republic). The samples were thermally demagnetized in an alternating-field demagnetizer with three posi-

tions of the specimen inside the AF coil whose magnetic field could vary within 0 to 100 mT under the shielded external field (Applied Physics Systems, United States). The specimens were 1-cm cubes.

The magnetic fraction composition analysis was conducted by magnetizing the specimens in the constant magnetic field up to their saturation, determining the remanent coercive force  $B_{cr}$ , and recording the magnetic hysteresis curves. In all samples, the saturation magnetization  $J_s$  was created in the field  $\sim 0.8$  T and then measured by the vibration magnetometer ORION (Russia). The measurements of remanent saturation magnetization  $J_{rs}$  were conducted by the JR-6 magnetometer. In the specimens for each volcano, the saturation curves  $J_{rs}$  were measured up to 0.5 T with a step of 0.05 T (Fig. 2a). In the same specimens, the opposite  $J_{rs}$  was created by the electromagnet (ORION, Russia) and the remanent coercive force  $B_{cr}$  was estimated (Fig. 2a). For each volcano, the magnetic hysteresis curves were recorded for one sample (Fig. 2c). The magnetic parameters are determined from the magnetic hysteresis curves with the correction for the paramagnetic background. All the studied basalt samples are magnetically strong. According to the measurements of the magnetic parameters from the magnetic hysteresis curves, the paramagnetic contribution in such strong basalt samples is below 5%; therefore, the allowance for the paramagnetic components barely changed the results. Nevertheless, in the samples for which the magnetic hysteresis curves were recorded the paramagnetic contribution was taken into account.

The domain state was estimated in the samples for which the magnetic hysteresis curves were recorded from the ratios  $J_{rs}/J_s$  and  $B_{cr}/B_c$ , where  $B_c$  is the coercive force. These ratios can be used individually; however, it is reasonable to use their combination (Evans and Heller, 2003) and visualize them in the Day plots (Fig. 2d) (Day et al., 1977). As the determination of the domain state, the following limits of the ratios  $J_{rs}/J_s$  and  $B_{cr}/B_c$  were accepted (Evans and Heller, 2003):  $J_{rs}/J_s \geq 0.5$ ,  $B_{cr}/B_c \leq 1.5$  for the single-domain (SD) grains;  $J_{rs}/J_s \leq 0.05$ ,  $B_{cr}/B_c \geq 4$  for the multidomain (MD) grains. For the pseudo-single domain grains we used the values of  $J_{rs}/J_s$  and  $B_{cr}/B_c$  that are intermediate between the indicated limits for the SD and MD grains.

Two types of thermomagnetic analysis (TMA) were conducted. In one version, TMA was carried out with the use of the vibration magnetometer from the temperature dependence of saturation magnetization  $J_s$  in the field of  $\sim 0.8$  T in the air atmosphere. In the second version, TMA was conducted by a two-component thermo-magnetometer (ORION, Russia) from the temperature dependence of the remanent saturation magnetization  $J_{rs}$  in the air atmosphere.

The degree of oxidation of the titanomagnetite grains was estimated from the value of the median alternating magnetic field  $B_{0.5}$  since the growth of  $B_{0.5}$  can be directly related to the changes in the titan-

magnetite composition or to the phase transformations of titanomagnetite (Kontny et al., 2003). For obtaining these estimates, the stability of NRM against the influence of the alternating magnetic field was studied in all the samples. For this purpose the curves of demagnetization by the alternating magnetic field up to a maximum of 100 mT with a step of 5 mT were recorded, and the value of the median magnetic field corresponding to the half of the remanent magnetization was measured (Fig. 2b).

For validating the composition of NRM carriers in the samples, petrographical-mineralogical investigations and microprobe analysis of the ore minerals were carried out. The measurements were conducted on the scanning electron microscope Cam Scan MV2300 at the Geological Institute of the Russian Academy of Sciences by operators N.V. Gor'kova and A.T. Savicheva and on the scanning electron microscope Jeol JSM-6480 LV in the Department of Geology of Moscow State University by operator E.V. Guseva.

In the iron-bearing and associated minerals, the composition of the central zones exposed by polishing and the composition of the unpolished parts of the volumetric grains that were picked manually was analyzed for all samples. Since the probe analysis does not estimate the Fe oxidation state, in the recalculations of the average titanomagnetite compositions for mineral chemistry, the standard proportion was assumed in all cases (two-thirds of  $Fe^{3+}$  and one-third of  $Fe^{2+}$ ) and the standard normalization coefficient of  $Fe^{2+}$  conversion to  $Fe^{3+}$  was taken into account.

The ore mineral analyses obtained for all the studied volcanoes correspond to titanomagnetite which, besides Fe and Ti, also contains insignificant amounts of Mg, Al, V, and Mn. If the amount of all the components in the analyses varied within close limits irrespective of the morphology of the mineral, the calculations were conducted with the average values determined for a given volcano. The theoretical formula of titanomagnetite was assumed as  $(Fe^{+2}, Mg, Ni, Zn, Mn)(Fe^{+3}, Ti)_2O_4$ .

A small amount of silica was detected in some analyses. The ore minerals are frequently coated by a glassy shell which is tightly stuck to their surface. It is assumed that during the analysis the beam breaks this shell and the analysis becomes contaminated by the additional silica; therefore, the chemical analyses of the ore material presented below, both from the thin sections and volumetric grains, were recalculated with the subtracted  $SiO_2$ .

It is also noted that the analysis in the thin sections sometimes detects slightly larger amounts of Mg, Mn, and Al in titanomagnetites. This is probably also due to capturing by the probe of the components from the paragenetic minerals and glass enclosing the titanomagnetite.

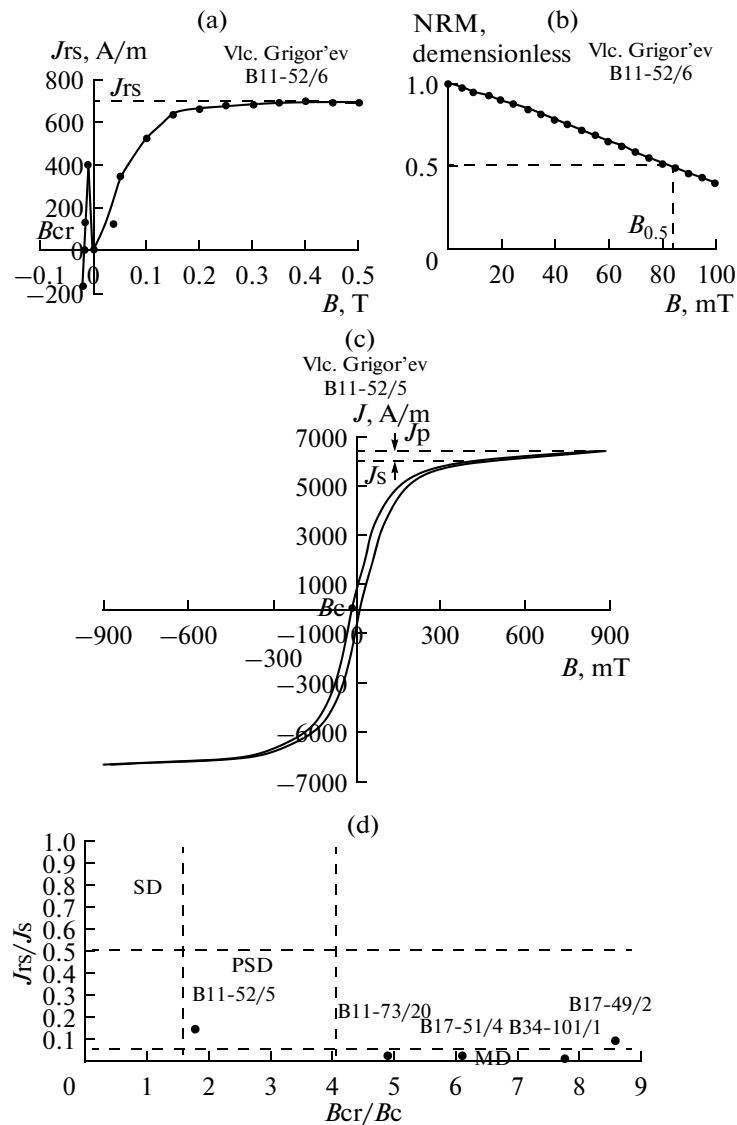


**Fig. 2.** The determination of the magnetic properties of the rocks by the examples of the dredged samples from the Grigor'ev submarine volcano: (a), the saturation curve of sample B11-52/6 in the constant magnetic field; (b), the NRM demagnetization curve of sample B11-52/6 in the alternating magnetic field; (c), the magnetic hysteresis curve for sample B11-52/5; (d), the Day diagram.

## RESULTS OF THE STUDY

### *The Grigor'ev Submarine Volcano*

The flat-topped Grigor'ev volcano (Fig. 1), named after the noted Russian geologist I.F. Grigor'ev (Bezrukov et al., 1958), is located 5.5 km northwest of Atlasov Island (the Alaid volcano) and rises from the depths of 800–850 m.

The basement of this volcano has coalesced with the basement of the Alaid volcano. The volcano covers an area of  $12.5 \times 15$  km along the basement and  $8.5 \times 11.5$  km along the isobath. The volcanic edifice has a volume of  $\sim 40$  km<sup>3</sup> (Babayants et al., 2005; 2006; Blokh et al., 2006a; 2006b; *Podvodnyi ...*, 1992). The summit of the submarine Grigor'ev volcano is cut by

the abrasion and leveled to a depth of 120–140 m which practically corresponds to the sea level in the Late Pleistocene. In the western and southwestern parts of the summit there are bedrock inliers rising to the depths of 50–55 m. They are probably an exhumed neck or, alternatively, they could have been formed after the formation of the summit and are the Holocene extrusion or small lava edifices.

The Grigor'ev submarine volcano is marked by an intense anomaly in the magnetic field  $\Delta T_a$  with an amplitude above 1400 nT. The volcanic edifice is magnetized in the direction of the present-day magnetic field; all the mentioned bedrock inliers are clearly manifest in the magnetic field  $\Delta T_a$  (Babayants et al., 2005; 2006; Blokh et al., 2006a; 2006b).

**Table 1.** Magnetic properties of the dredged rocks composing the undersea volcanoes on the Sea-of-Okhotsk slope within the northern part of KIA

Rock	Number of samples	Range of variations in natural remanent magnetization NRM, A/m	Range of variations in magnetic susceptibility, $k \times 10^{-3}$ , SI units
1	2	3	4
Grigor'ev submarine volcano			
Crystallized basalts	3	1.57–1.94	2.39–8.29
Porphyry basalts	9	4.12–18.90	18.34–29.77
Aphyric basalts	3	13.61–28.45	24.12–94.83
Tuffite	1	1.47	2.42
1.4 submarine volcano			
Andesibasalt	5	0.22–7.35	16.67–44.84
Daciandesites	4	0.98–1.89	23.74–50.74
Belyankina submarine volcano			
Olivine basalts	10	0.15–29.01	10.50–70.96
Smirnov submarine volcano			
Andesibasalts	5	0.42–4.12	18.96–38.19
Andesites	2	3.10–5.64	2.03–3.34
Dacites		0.40–0.82	16.02–22.16
Edelshtein submarine volcanic massif			
Andesibasalts	7	1.53–50.13	16.29–48.46
Andesites	4	0.63–2.24	47.35–53.99
Daciandesites	1	0.68	48.46

The dredging of the Grigor'ev volcano (*Podvodnyi ...*, 1992) has lifted single-type seabed basalts rich in silica, iron, and potassium, with a medium Ti content (tables 1 and 2). The NRM in the dredged basalts varies from 1.57 to 28.45 A/m;  $k$  lies within  $(2.39–94.83) \times 10^{-3}$  SI units (Table 1).

Two samples of the porphyric basalts (B11-52/5 and B11-52/22) and one sample of the aphyric basalt were subjected to rock magnetic studies (Table 3). The stepwise isothermal magnetization of the basalt sample B11-52/6 in the constant magnetic field has shown that the specimen is saturated at 0.25 T. All the three specimens are magnetically isotropic. The magnetization is due to the high content of the low-coercive ( $B_{cr} = 17–26$  mT) PSD ferromagnetic grains. Samples B11-52/5 and B11-52/6 have the higher NRM values and a larger median magnetic field than sample B11-52/22. This may indicate that samples B11-52/5 and B11-52/6 have got crystallized in the marginal parts of basalt flows under the rapid cooling of the melt (*Priroda ...*, 1996).

The TMA from  $J_r(T)$  of the aphyric basalt sample B11-52/6 has shown that the curve of the first heating has a smooth bend at  $\sim 250^\circ\text{C}$ ; the magnetization is completely destroyed at  $\sim 500^\circ\text{C}$ . The curve for the second heating goes above the first-heating curve and generally follows it; the remanent magnetization is

removed at  $\sim 550^\circ\text{C}$ . The curve of the second heating retains the bend which is however shifted here towards the higher temperatures ( $\sim 300^\circ\text{C}$ ). Hence, the remanent magnetization is mainly carried by the PSD titanomagnetite grains (Table 3) with different Ti content. During the heating the specimen underwent heterophase transformation which resulted in the formation of two components, Ti-rich and Ti-depleted ones. The growth of the magnetization in the curve of the second heating is due to the formation of titanomagnetite with lower Ti-content compositionally close to magnetite and with a higher value of spontaneous magnetization.

In the heating curve of TMA from  $J_s(T)$  for the twin specimen of aphyric basalt B11/52/6 the bend is observed at  $\sim 490^\circ\text{C}$  (Fig. 4). The cooling curve is irreversible and has two inflections at 530 and  $280^\circ\text{C}$  indicating the formation of two magnetic phases corresponding to titanomagnetite with high and low Ti content.

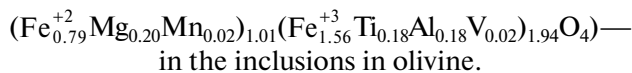
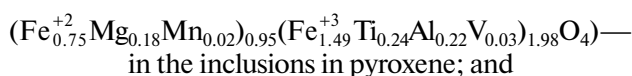
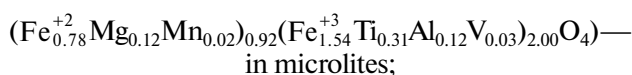
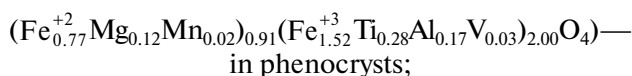
The petrographical investigation and microprobe analysis of samples B11-52/5 and B11-52/6 identified the studied specimens as olivine-pyroxene-plagioclase basalts, large-grained porphyry (Fig. 5) with small variations in the proportion of the phenocrysts and the groundmass (the phenocrysts to groundmass ratio is 3/1 in B11-52/5 and 4/1 in B11-52/22). Phenocrysts have sizes ranging from 0.5 to 4mm, are dominated by

**Table 2.** The stations of dredging the submarine volcanoes on the Sea-of-Okhotsk slope of the northern part of KIA

No.	Dredge no.	Dredging point coordinates		Dredging depth interval, m
		latitude, N	longitude, E	
Grigor'ev submarine volcano				
1	B11-52	50°56.5'	155°25.6'	120–87
1.4 submarine volcano				
2	B34-101	50°20.4'	154°11.6'	1100–700
3	B40-32/7	50°20.8'	154°12.3'	770–615
Belyankina submarine volcano				
4	B11-72	49°56.2'	154°07.7'	720–660
5	B-17-49	49°56.2'	154°09.1'	850–750
Smirnov submarine volcano				
6	B11-73	49°54.4'	154°20.4'	1300–1050
Edelshtein submarine volcanic massif				
7	B17-51	49°12.8'	153°29.0'	2200–740
8	B40-26	49°10.8'	153°27.2'	1350–980

plagioclase and minor amounts of pyroxene, olivine, and ore mineral. The groundmass glass is crystallized up to 50%. Among microlites, pyroxene and plagioclase are prevalent.

The bulk content of ore mineral in sample B11–52/5 is ~10% of the volume of the rock; in sample B11–52/22, it is ~15%. Ore mineral is present in the rock in the form of phenocrysts, microlites, and inclusions in pyroxene and olivine. In all cases its crystallochemical composition corresponds to titanomagnetite:



According to these formulas, the Ti-content in titanomagnetites varies from 0.24 to 0.31 formula units (f.u.) with the anomaly of 0.18 f.u. for the inclusions in olivine which have been first to have crystallized even from the primary melt. They have the maximal iron content. Next, the inclusions in pyroxene were segregated ( $X = 0.24$  f.u.), then the individual large titanomagnetite phenocrysts were crystallized ( $X = 0.28$  f.u.). Finally, the microlites were segregated at the lowest temperatures and, judging by the structure of the texture of the groundmass, in the near-surface conditions ( $X = 0.31$  f.u.). They have the maximal Ti content.

The microprobe analysis of the aphyric basalt sample B11–52/6 enabled the Ti-content to be estimated. The Ti/Fe mass ratio varies within 0.09–0.14 which corresponds, within the first approximation, to the Ti-content in titanomagnetite  $X \sim 0.28$ –0.42 and the Curie points in the interval  $T_c \sim 270$ –370°C.

The calculated Curie points are lower than the Curie point measured in the experiment from  $J_s(T)$  and reasonably closely coincide with the blocking temperature according to  $J_r(T)$ , which points to the oxidized titanomagnetite (titanomaghemite) as the main magnetic mineral carrier of NRM.

#### *Submarine Volcano 1.4*

The submarine sharp-summit volcano 1.4, which was discovered in 1989 during the 34th cruise of Vulkanolog ORV (Rashidov et al., 1992), is located 80 km west of Paramushir Island (Fig. 1).

It rises 650–700 m above the adjacent seafloor. Its basal contour is slightly elongated northwest and has a size of  $\sim 6.5 \times 7$  km. The summit is complicated by a number of peaks. A negative topographic form encircles the volcano's base by almost a closed ring-shaped rim. The volume of the edifice is  $\sim 13 \text{ km}^3$  (Bondarenko et al., 1994; Rashidov et al., 1992).

The volcanic edifice manifests itself by a positive magnetic anomaly with an amplitude of 400–500 nT. A local peak reaching 700 nT is observed in the distribution of the magnetic field near the volcano's apex. The maximum of the anomaly is offset to the south of the volcano's summit, which testifies to the normal magnetization of the rocks composing the volcano

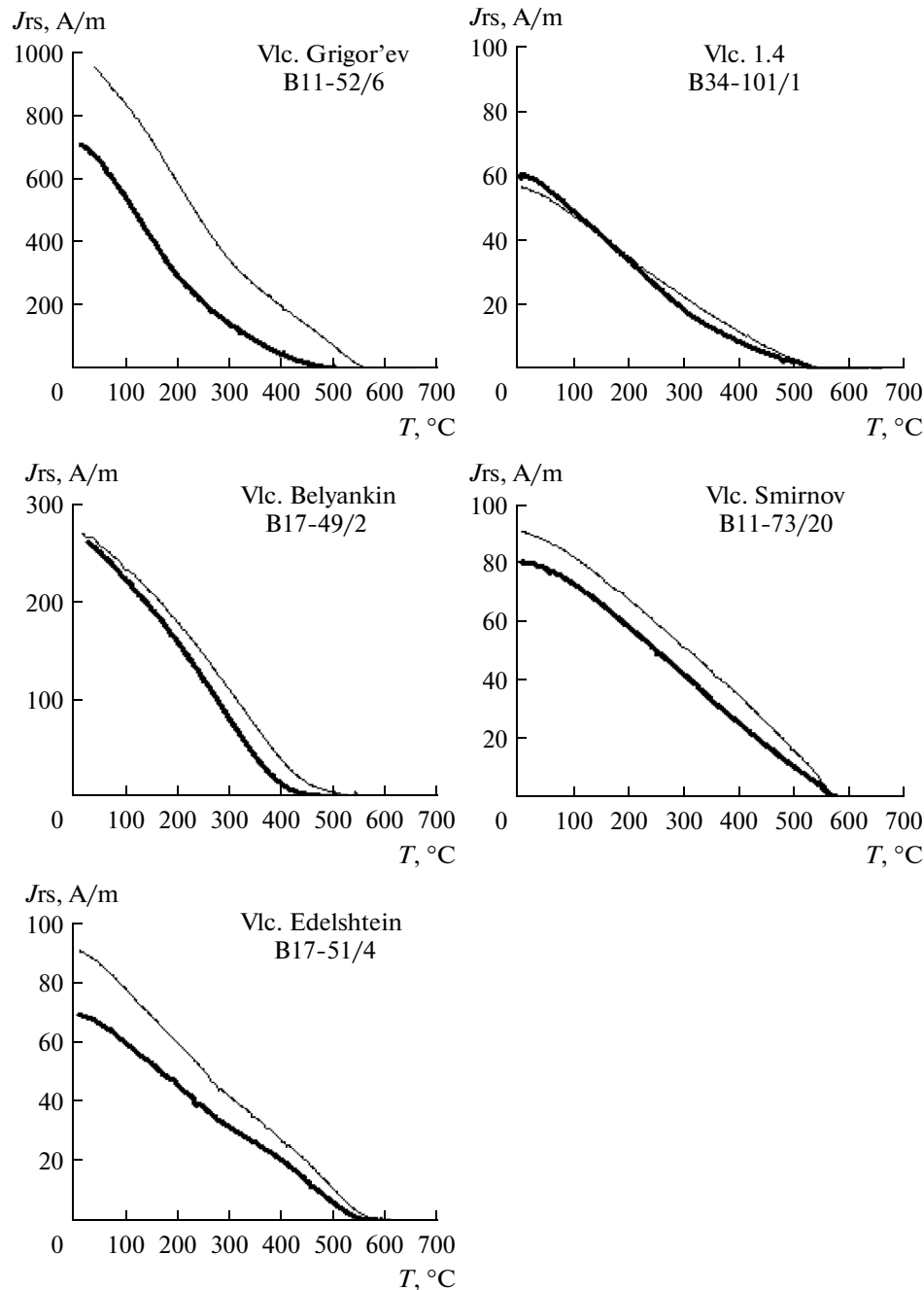


**Fig. 3.** The thermomagnetic curves depicting the dependence of remanent saturation magnetization  $J_{rs}$  on temperature  $T$ . The heavy and the thin lines correspond to the first and second heatings, respectively.

(Babayants et al., 2005; 2006; Bondarenko et al., 1994).

The dredging from the near-summit part of the volcano has mainly brought up amphibole andesibasalts with monoclinic pyroxene andesibasalts and plagiobasalts, as well as Daciandesites (Bondarenko et al., 1994; Rashidov et al., 1992) (Tables 1 and 2). Rare clasts of granitoids and andesite pumice, minor amounts of scoria, sedimentary pebbles, iron-manganese items, and seabed biota are present (Anikieva et al., 2008; Bondarenko et al., 1994).

The NRM of andesibasalts varies within 0.22–7.35 A/m and  $k$ , within  $(16.67–44.84) \times 10^{-3}$  SI units. In dacites, NRM ranges from 0.98 to 1.89 A/m and  $k$ , within  $(23.74–50.74) \times 10^{-3}$  SI units (Table 1).

The rock magnetic studies were conducted for two porphyric andesite-basalt samples B34-101/1 and B40-32/7 (Table 3). The magnetization of the first sample is due to the presence of relatively large MD grains of low-coercive magnetic mineral ( $B_{cr}$ ) = 17 mT. The magnetization of the second sample is determined by the presence of the PSD grains of the magnetic

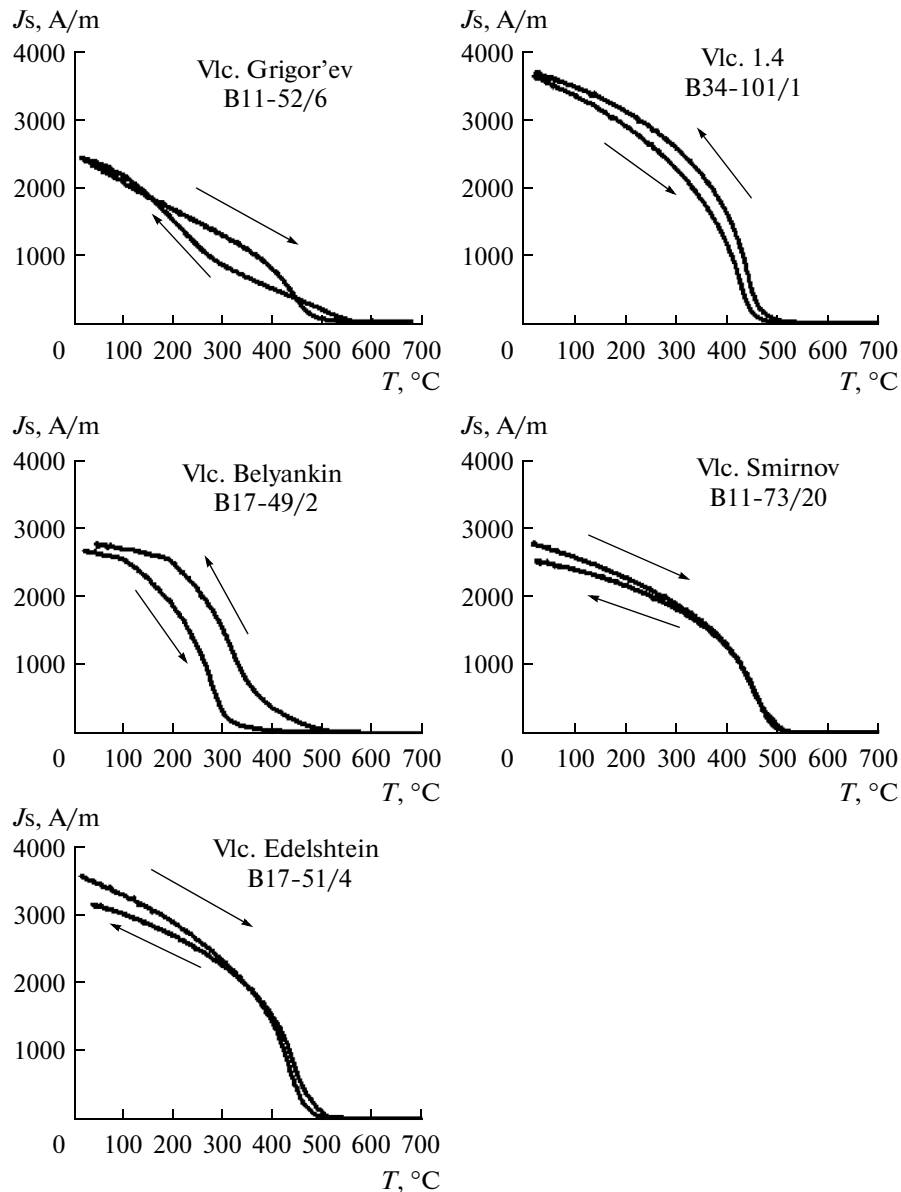


Fig. 4. The thermomagnetic curves depicting the dependence of remanent magnetization  $J_s$  on temperature  $T$ . The arrows show the heating–cooling cycle.

material, which is also low coercive ( $B_{cr} = 18$  mT). In the tested samples, AMS is absent; the specimens are magnetically soft, and NRM is easily destroyed by the alternating magnetic field.

The TMA from  $J_{rs}(T)$  of sample B34-101/1 has shown that the magnetization is completely removed at  $\sim 550^\circ\text{C}$  (Fig. 3). The thermomagnetic curve of the second heating virtually coincides with the curve of the first heating and also has a single blocking temperature of about  $550^\circ\text{C}$ . In this sample, the magnetization is largely carried by the heating-resistant titanomagnetite compositionally close to magnetite.

The TMA from  $J_s(T)$  for the twin specimen of B34-101/1 revealed a bend at  $\sim 460^\circ\text{C}$  in the TMA curve of the first heating (Fig. 4). The cooling curve goes

slightly above the curve of the first heating and generally follows it; its bend point is shifted towards the higher Curie points ( $\sim 480^\circ\text{C}$ ).

The fact that the Curie point and blocking temperature in the different analyses do not coincide could probably be due to the fact that TMA from  $J_{rs}(T)$  is sensitive to small magnetic grains, whereas TMA from  $J_s(T)$  rather highlights large magnetic grains (D.M. Pechersky, oral communication). Hence, the TMA from  $J_s(T)$  in this sample revealed the presence of the heating resistant titanomagnetite grains with the Curie points  $\sim 460^\circ\text{C}$ .

The petrographical studies and microprobe analysis of the B34-101/1 sample identified it as porphyry andesibasalt of the amphibole-two-pyroxene-plagioclase

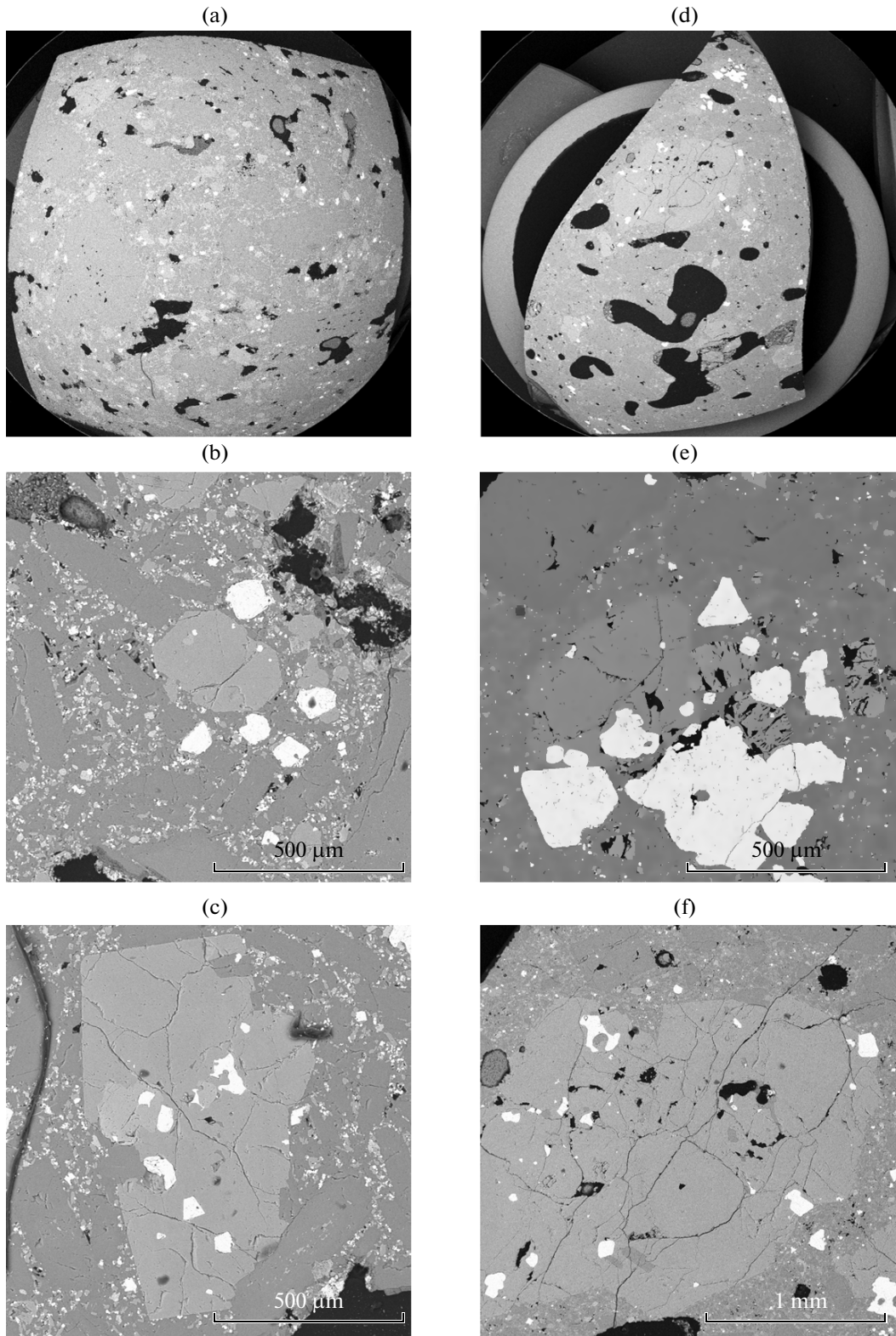


**Fig. 5.** Titanomagnetites from the Grigor'ev submarine volcano: (a)–(c), sample B11-52/22; (d)–(f), sample B11-52/5. (a), (d), the overall view of the thin sections. The dimensions of the gas voids and their distribution in the sections as well as the number, size, and density of occurrence of the titanomagnetite grains (bright white point and larger precipitates) are clearly visible; (b), (e), titanomagnetite phenocrysts and microlites in the rock. It can be seen that the groundmass of the thin section of sample B11-52/22 contains much more microlites than in the thin section of the B11-52/5 sample; (c), (f), the titanomagnetite inclusions in the large pyroxene phenocrysts.

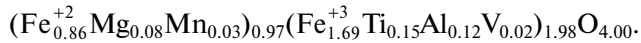
**Table 3.** The rock magnetic characteristics of the dragged samples of the rocks composing the submarine volcanoes on the Sea-of-Okhotsk slope of the northern part of KIA

No.	Sample no.	Sample description	NRM, A/m	$k \times 10^{-3}$ , SI units	$Q_n$	$P'$	$B_{cr}$ , mT	$B_{0.5}$ , mT	$J_s$ , A/m	$J_{rs}/J_s$	$B_{cr}/B_c$	Domain structure	C, %
Grigor'ev submarine volcano													
1	B11-52/5	Porphyric basalt	18.9	49.41	9.61	1.019	26	70	6000	0.14	1.78	PSD	1.7–1.8
2	B11-52/6	Aphyric basalt	15.31	20.09	19.14	1.017	17	85	2450	0.29		PSD	
3	B11-52/22	Porphyric basalt	4.12	50.4	2.05	1.017	22	35	7460	0.07		PSD	
1.4 submarine volcano													
4	B34-101/1	Porphyric andesibasalt	0.22	39.49	0.14	1.027	17	15	3600	0.01	7.76	MD	0.9
5	B40-32/7	Porphyric andesibasalt	4.27	16.67	6.43	1.010	18	27	2260	0.1		PSD	
Belyankina submarine volcano													
6	B11-72/3	Porphyric basalt	22.48	44.38	12.72	1.023	43	>100	1280	0.27		PSD	
7	B17-49/2	Porphyric basalt	7.33	39.18	4.7	1.028	53	>100	2800	0.1	8.62	MD (?)	0.8
8	B17-49/5	Porphyric basalt	0.15	10.50	0.36	1.064	23	92	1330	0.04		MD	
Smirnov submarine volcano													
9	B11-73/8	Porphyric andesibasalt	0.53	30.23	0.44	1.018	20	14	4720	0.06		PSD	
10	B11-73/10	Subaphyric dacites	0.54	20.00	0.68	1.058	21	33	2110	0.01		MD	
11	B11-73/20	Aphyric andesibasalt	0.42	38.19	0.28	1.093	18	57	2700	0.03	4.92	MD	0.6–0.7
Edelshstein submarine volcanic massif													
12	B17-51/2	Porphyric andesibasalt	1.53	42.46	0.91	1.034	18	27	4410	0.02		MD	
13	B17-51/4	Porphyric andesibasalt	1.70	39.3	1.09	1.056	18	28	3500	0.02	6.10	MD	0.8–0.9
14	B17-51/8	Aphyric andesibasalt	31.56	19.23	41.23	1.029	28	100	2860	0.16		PSD	
15	B40-26/2	Porphyry daciandesite	0.68	48.46	0.35	1.049	17	9	4540	0.01		MD	
16	B40-26/3	Aphyric andesibasalt	10.18	16.29	15.70	1.012	41	>100	2490	0.17		PSD	

NRM is natural remanent magnetization;  $k$  is magnetic susceptibility;  $Q_n$  is Koenigsberger ratio;  $P'$  is the degree of anisotropy of magnetic susceptibility;  $B_{cr}$  is remanent coercive force;  $B_{0.5}$  is median magnetic field;  $B_c$  is coercive force;  $J_{rs}$  is remanent saturation magnetization;  $J_s$  is saturation magnetization; PSD stands for pseudo-single-domain grains; MD stands for multidomain grains; C is bulk concentration of ferrimagnetic.

clase composition, with olivine and titanomagnetite. The sample is highly porous; the pores make up 10–13% of the total volume of the rock (Fig. 6a). The phenocrysts/groundmass ratio is 3/1. The ore mineral distribution in the rock (in thin sections) and the morphology of the phenocrysts and microlites are clearly distinct in Fig. 6a. The volumetric crystal is shown in Fig. 6d.

The chemical composition of the ore minerals is presented in Table 4. Here, the chemistry of phenocrysts, microlites, and other morphological forms of the mineral in the andesibasalt of volcano 1.4 practically coincides; therefore, the recalculation into formulas was done for the combined average composition (from 19 analyses):



It can be seen that the crystal lattice of the mineral, compared to its theoretical composition, is somewhat deficient in both the trivalent and bivalent cations; however, the natural occurrence of this slightly cation-deficient mineral is real. According to the calculations, the Ti-content in the unit mineral cell is  $X = 0.15$  f.u., whereas the variations in the Ti-content in the micro- and macro-grains was  $X = 0.13$ – $0.17$  f.u. which corresponds to the Curie points in the interval  $T_c = 450$ – $480^\circ\text{C}$  accommodating the Curie points estimated in the experiment from TMA  $J_s(T)$ . Hence, the main NRM carriers in the sample are the low-Ti titanomagnetite grains.

### The Belyankin Submarine Volcano

The Belyankin submarine volcano, named after the noted Soviet petrographer academician D.S. Belyankin (Bezrukov et al., 1958) is located 23 km northwest of Makanrushi Island (Fig. 1).

The Belyankin volcano has a shape of isometric cone and rises to about 1100 m above the neighboring seabed. The sharp summit of the volcano is located at a depth of 508 m. The size of the volcanic edifice at the base is  $9 \times 7$  km and its area is  $\sim 50$  km<sup>2</sup> (*Podvodnyi ...*, 1992; Rashidov and Bondarenko, 1998).

The Belyankin volcano is clearly expressed in the magnetic field  $\Delta T_a$  by the anomaly of up to 650 nT peaking southeast of the volcano's apex. The volcanic edifice has normal magnetization (Rashidov and Bondarenko, 1998).

The dredging of the Belyankin submarine volcano has brought up homogeneous porphyric olivine basalts (Kichina and Ostapenko, 1977; Ostapenko and Kichina, 1982; *Podvodnyi ...*, 1992) (Tables 1 and 2). The NRM of the dredged rocks varies from 0.15 to 29.01 A/m and  $k$  ranges within  $(10.50$ – $70.96) \times 10^{-3}$  SI units (Table 1).

Three samples of the dredged porphyric basalts were studied by the rock magnetic analysis methods (Table 3). The samples demonstrate the scatter in

NRM within 0.15 to 22.48 A/m. The value of  $k$  increases with the growth in NRM which indicates the increase in the concentration of the NRM-carrier mineral grains.  $P'$  reaches 1.064; the remanent coercive force  $B_{cr}$  is 23–53 mT. All the porphyry basalt samples have a high magnetic rigidity ( $B_{0.5} \geq 92$  mT). The sizes of the magnetic grains fall in the PSD–MD interval.

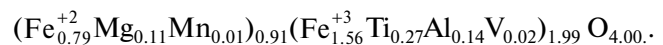
The TMA from  $J_r(T)$  of the porphyric basalt sample B17-49/2 (Fig. 3) shows that the magnetization is mainly carried by the magnetic mineral with the blocking temperature at  $\sim 410^\circ\text{C}$ . The curve of the second heating follows the first-heating curve slightly above it and has a bend at  $\sim 440^\circ\text{C}$ . The magnetization in this sample is mainly carried by titanomagnetite with Ti ( $X = 0.22$ ). The slow cooling resulted in the formation of two magnetic mineral phases—Ti-rich and Ti-depleted ( $X \sim 0.18$ ). The TMA analysis has captured exactly the formation of the second phase.

The curve of the first heating in TMA from  $J_s(T)$  for the twin specimen of the porphyric basalt sample B17-49/2 (Fig. 4) also has a single magnetic phase with the Curie point at  $\sim 320^\circ\text{C}$ . The  $T_c$  point on the cooling curve is shifted towards the higher temperatures to  $360^\circ\text{C}$ ; the cooling curve goes above the heating curve, which indicates the formation of the low-Ti magnetic phase.

The petrographical and microprobe investigation of the B17-49/2 sample identified it as olivine-two-pyroxene-plagioclase porphyric basalt with the glassy groundmass substituted by fine-dispersed ore material and converted into opacite (Figs. 7a and 7b). Gas voids ( $\sim 20\%$  of the volume of the rock) determining the high porosity of basalt are present. The phenocrysts and groundmass are nonuniformly distributed across the area of the thin section. The predominant phenocrysts/groundmass ratio is 3/1; however, also the segments with rarer phenocryst occurrences (with phenocrysts to ground mass ratio of 2/2) are observed.

The ore mineral content is 15%. The ore mineral is often present in the form of inclusions in olivine and pyroxene.

The chemical composition of the ore mineral in the material dredged from the Belyankin volcano is presented in Table 4. No significant distinctions in the chemical compositions of the different morphological types of the ore mineral are found. The recalculation of the average (over 13 analyses) composition gives the following mineral formula:



This formula demonstrates a significant deficiency of bivalent cations; however, the occurrence of such a structurally-defective mineral is feasible. The calculated mean Ti content per unit cell is  $X = 0.27$  f.u. The variations in the Ti content in the micro- and macro-grains are  $X = 0.23$ – $0.29$  f.u., which corresponds to the interval of the Curie points of  $\sim 360$ – $410^\circ\text{C}$  accommodating the empirical Curie points deter-

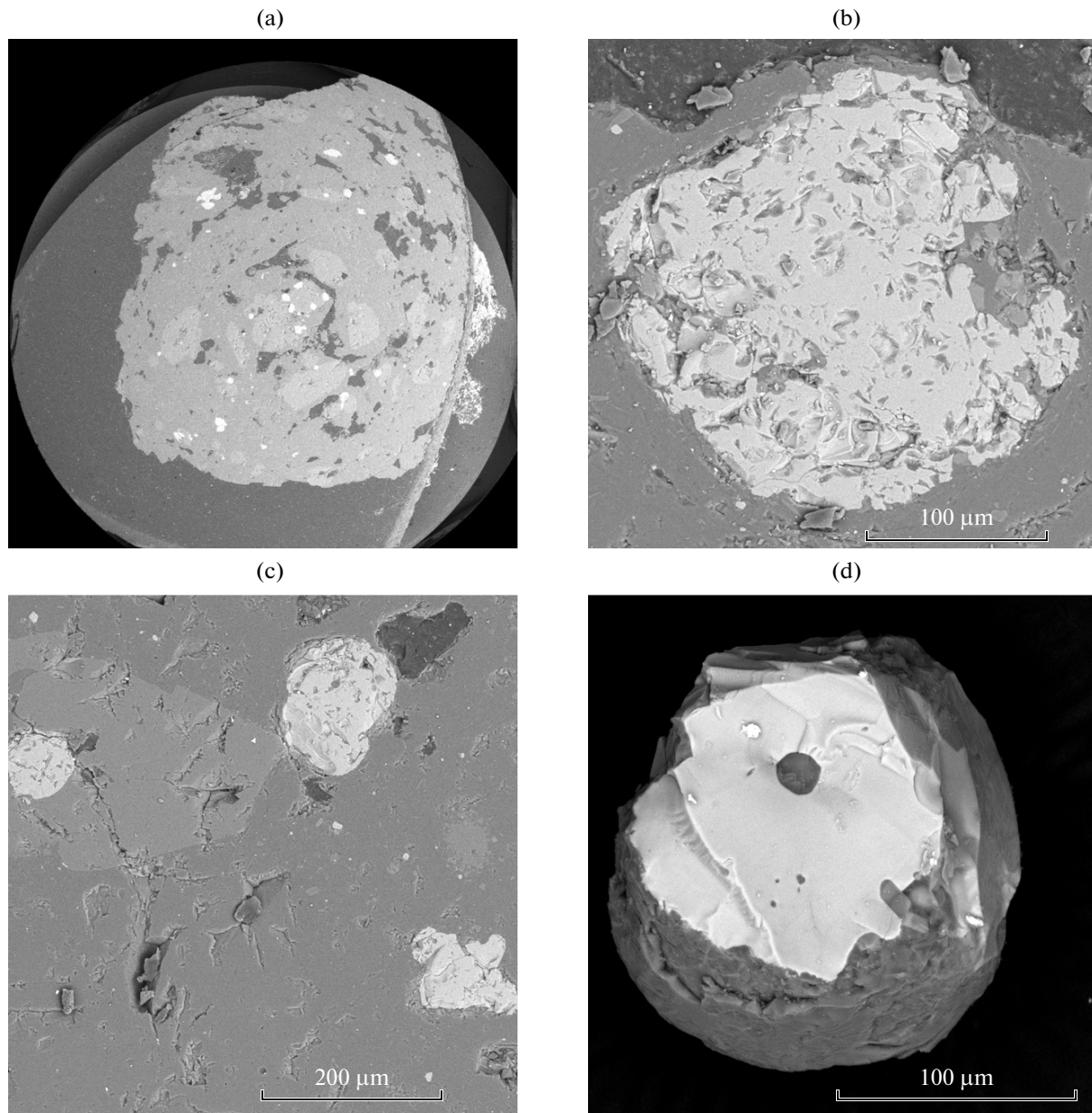


**Fig. 6.** Titanomagnetites from the 1.4 submarine volcano (sample B34-101/1): (a), the overall view of the thin section. The rock is macro- and microporous, with nonuniformly distributed gas voids; titanomagnetite phenocrysts and microlites (bright white points and spots) are nonuniformly distributed across the section; (b), titanomagnetite phenocryst: uneven, dislocated surface of the crystal is clearly seen; (c), titanomagnetite microlites (white precipitates and points). The extreme left grain is the inclusion in the pyroxene crystal; the remaining (including the micron-sized point precipitates) is distributed across the groundmass of the rock; (d), the volumetric crystal of titanomagnetite (white) coated with a tightly stuck film of the glassy groundmass.

mined by TMA. Hence, the main magnetization carrier in the porphyry basalt sample B17-49/2 is unaltered titanomagnetite.

Besides titanomagnetite, also very rare pyrite crystals with a size of up to 10  $\mu\text{m}$  and adhesions of probably native Cu, Zn, and Ag with the sizes of up to the first few  $\mu\text{m}$  (Figs. 7c and 7d) are detected. The small sizes of these occurrences only allow qualitative assessment of their composition. Apatite is present.

#### *The Smirnov Submarine Volcano*

The flat-topped Smirnov volcano, named after the notable Soviet geologist academician S.S. Smirnov (Bezrukov et al., 1958), is located 12 km north-northwest of Makanrushi Island (Fig. 1). Its base at a depth level of  $\sim 1800$  m coalesces with the base of Makanrushi Island. The flat summit is at a depth of 950 m.

The  $8 \times 11$  km base of the volcano has an area of  $\sim 70$  km<sup>2</sup>. The volcanic edifice at the level of the sum-

mit has a size of  $2 \times 3$  km. The relative height of the edifice is 850 m and the volume is  $\sim 20 \text{ km}^3$  (Podvodnyi ..., 1992; Rashidov and Bondarenko, 1998).

The Smirnov volcano creates a magnetic anomaly  $\Delta T_a$  with an amplitude of 470 nT. The edifice is magnetized in the direction of the present-day magnetic field (Rashidov and Bondarenko, 1998).

The dredging of the Smirnov volcano has delivered various rocks compositionally varying from basalts to dacites (Ostapenko, 1976; 1978; Ostapenko and Kichina, 1977; 1982; Podvodnyi ..., 1992) (Tables 1 and 2). The NRM of the dredged andesibasalts is 0.42–4.12 A/m; in andesites, 3.10–5.64 A/m; in dacites, 0.40–0.82 A/m. The  $k$  values in these rocks vary within  $(18.96\text{--}38.19) \times 10^{-3}$ ,  $(2.03\text{--}3.34) \times 10^{-3}$ , and  $(16.02\text{--}22.16) \times 10^{-3}$  SI units, respectively (Table 1).

The rock magnetic analysis was carried out for three dredged samples (porphyric andesibasalts B11-73/8, subaphyric dacites B11-73/10, and aphyric andesibasalt B11-73/20) (Table 3). All of them have relatively low NRM = 0.42–0.53 A/m and rather high  $k = (20\text{--}38) \times 10^{-3}$  SI units, which may indicate the high concentration of the NRM-carrier mineral grains. The degree  $P'$  in these samples varies within 1.018 to 1.093. The magnetization of the samples is due to the presence of the PSD- and MD-grains of a low-coercive magnetic mineral ( $B_{cr} = 18\text{--}21$  nT). The magnetization is unstable against an alternating magnetic field ( $B_{0.5} = 14\text{--}57$  nT).

The TMA from  $J_{rs}(T)$  for the B11-73/20 aphyric andesibasalts (Fig. 3) shows that both the first- and second-heating curves have recorded a blocking temperature corresponding to the Curie point of magnetite  $\sim 575^\circ\text{C}$ . The curve of the second heating follows the curve of the first heating and is located slightly above it. Hence, the main carrier of the magnetization in this sample is magnetite.

The TMA from  $J_s(T)$  for the twin specimen of the aphyric andesibasalts B11-73/20 (Fig. 4) has demonstrated the presence of a single Curie point at  $\sim 500^\circ\text{C}$ . The heating and cooling curves coincide and are practically reversible. The discrepancies in the results of estimating the blocking temperature from the  $J_{rs}(T)$  and the Curie point from  $J_s(T)$  can probably be due to the nonuniform distribution of the ferrimagnetic grains and, hence, significant scatter among the grains by their Curie points and blocking temperature in the studied samples. A similar situation is also noted in (Trukhin et al., 2006). The fact that the blocking temperature differs from the Curie points determined by the different analyses can also be associated with the different sensitivity of the TMA from  $J_{rs}(T)$  and TMA from  $J_s(T)$ , which are likely to mainly recognize the smaller and larger grains, respectively, as noted above. Hence, the analysis suggests that the NRM in the sample B11-73/20 is mainly carried by the heating-resistant low-Ti titanomagnetite compositionally close to magnetite.

**Table 4.** The variations and average composition of titanomagnetites in the rocks composing the submarine volcanoes on the Sea-of-Okhotsk slope in the northern part of KIA

Mineral species	Maximal content	Minimum content	Average content
Grigor'ev volcano (34 analyses)			
MgO	6.07	0.94	2.96
Al <sub>2</sub> O <sub>3</sub>	7.23	0.71	4.08
TiO <sub>2</sub>	17.01	2.51	10.36
V <sub>2</sub> O <sub>5</sub>	1.95	0	1.25
MnO	1.41	0	0.78
FeO	88.33	74.82	80.57
Volcano 1.4 (19 analyses)			
MgO	3.96	0.24	1.47
Al <sub>2</sub> O <sub>3</sub>	5.16	1.62	2.94
TiO <sub>2</sub>	9.27	4.97	5.89
V <sub>2</sub> O <sub>5</sub>	1.24	0.53	0.81
MnO	1.42	0.43	0.96
FeO	90.95	82.33	87.86
Belyankin volcano (13 analyses)			
MgO	5.16	0.03	2.1
Al <sub>2</sub> O <sub>3</sub>	6.25	0.82	3.41
TiO <sub>2</sub>	14.51	8.34	10.54
V <sub>2</sub> O <sub>5</sub>	1.87	0	0.86
MnO	1.09	0	0.48
FeO	86.2	80.2	82.58
Smirnov volcano (19 analyses)			
MgO	2.22	0	1.13
Al <sub>2</sub> O <sub>3</sub>	5.46	0.07	2.45
TiO <sub>2</sub>	6.41	2.97	5.56
V <sub>2</sub> O <sub>5</sub>	1.34	0	0.59
MnO	1.38	0.25	0.87
FeO	92.4	85.75	89.38
Edelshtein volcano (16 analyses)			
MgO	2.69	0.16	1.21
Al <sub>2</sub> O <sub>3</sub>	3.87	0.69	2.24
TiO <sub>2</sub>	12.62	4.66	6.18
V <sub>2</sub> O <sub>5</sub>	0.95	0	0.57
MnO	1.49	0.29	0.92
FeO	92.19	85.07	88.88

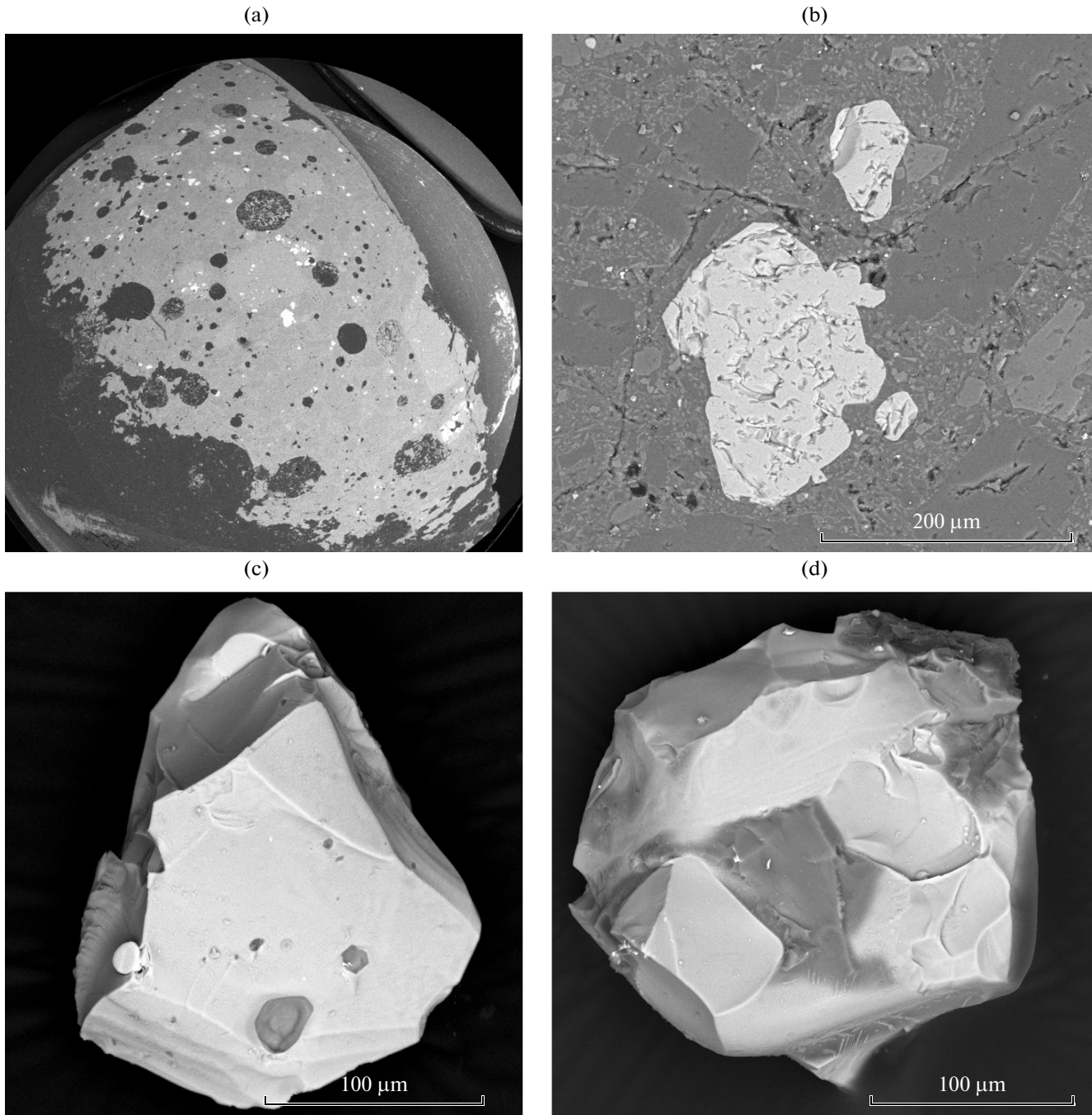


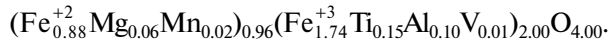
**Fig. 7.** Titanomagnetites from the Belyankin submarine volcano (sample B17-49/2): (a), the overall view of the thin section. The distribution of the gas voids having different sizes and the titanomagnetite phenocrysts and microlites (bright white spots and points); (b) the titanomagnetite phenocrysts with different sizes, surrounded by the groundmass and located close to the pyroxene and plagioclase phenocrysts; titanomagnetite microlites (small white points) are dispersed in the ambient environment; (c) the volumetric crystal of titanomagnetite with the apatite inclusions (dark gray within white), with the intergrowth with a small pyrite crystal (white “bead” on the left edge); (d), the volumetric crystal of titanomagnetite: in the frontal dark gray zone of the glassy groundmass there are small white points which are interpreted as silver.

The petrographical investigations and microprobe analysis of the B11-73/20 sample showed that it is plagioclase-hornblende large-grain porphyry andesibasalt with ore mineral and single signs of olivine, pyroxene, and biotite. The phenocryst/groundmass ratio is

50/50. Andesibasalt contains up to 15% xenoliths of the fully crystallized weakly porphyritic two-pyroxene-hornblende (probably with olivine) basalt. The xenolith clasts are up to  $4 \times 4$  mm in size. The ore mineral has a size up to  $0.4 \times 0.4$  mm in phenocrysts and

0.04 × 0.04 mm in the groundmass. Titanomagnetite phenocrysts are predominant; titanomagnetite intergrowths in pyroxene occur. This is most typical of the xenolith segments.

The ore mineral distribution in the rock (across the thin section) and the morphology of the phenocrysts and microlites are clearly seen in Figs. 8a–8c. The volumetric crystal is shown in Fig. 8d. The chemical compositions of the ore minerals are presented in Table 4. The titanomagnetite formula obtained by recalculating from the average (over 18 analyses) mineral composition has the following form for the titanomagnetites from the Smirnov volcano:



It can be seen that, compared to the theoretical mineral composition, there is a slight deficiency of bivalent cations in the crystal lattice. The average Ti-content per unit mineral cell is estimated at  $X = 0.15$  f.u. The variations in the Ti-content in the micro- and macrograins are  $X = 0.14–0.16$  f.u., which correspond to the Curie points in the  $\sim T_c = 490–510^\circ\text{C}$  interval accommodating the experimental Curie points estimated from TMA  $J_s(T)$ .

However, the mentioned xenoliths may have a different ore mineral composition (the presence of ilmenite has not been excluded).

#### *The Edelshtein Submarine Volcanic Massif*

The submarine volcanic massif named after the noted Soviet geologist–geomorphologist professor Ya.S. Edelshtein (Bezrukov et al., 1958) is located ~26 km north of Chirinkotan Island (Fig. 1).

The Edelshtein volcanic massif is formed by two merged closely spaced volcanic edifices with sharp apices. The edifices, the northeastern and southwestern ones, rise to depths of 620 and 840 m, respectively. By size, the northeastern edifice is much larger than the southwestern one. The distance between the edifices is about 5 km; the saddle between them rises to a depth of ~1300. The total height of the volcanic massif, together with its buried part, is ~2600 m. Across the base, the volcanic massif has a size of 19 × 25 km; the volume is ~315 km<sup>3</sup> (Podvodnyi ..., 1992; Rashidov and Bondarenko, 2003).

The Edelshtein massif is expressed in the anomalous magnetic field  $\Delta Ta$  by a distinct local anomaly trending northeast. The anomalies corresponding to the southwestern and northeastern edifices reach the peak values of 1060 and 850 nT, respectively. The maximal gradient of the magnetic field is as high as 350 nT/km (Brusilovskii et al., 2004; Rashidov and Bondarenko, 2003).

The dredging of the northeastern edifice of the Edelshtein massif has brought up amphibole-plagioclase andesites, andesibasalts, and daciandesites (Korenev et al., 1982; Podvodnyi ..., 1992; Rashidov and Bondarenko, 2003) (Table 1). The dredging of the

southwestern edifice delivered olivine–clinopyroxene–plagioclase basalts, rare–porphyric dense olivine–plagioclase andesibasalt, porous pyroxene–plagioclase andesites, and a lesser amount of daciandesites. Some samples have iron–manganese crusts (Anikieva et al., 2008).

The dredged rocks strongly differ by NRM and  $k$ . The NRM varies within 1.53–50.13 A/m in andesibasalts and 0.63–2.24 A/m in andesites; it is 0.68 A/m in the daciandesite sample. The  $k$ -values range within  $(16.29–48.46) \times 10^{-3}$  SI units in andesibasalts and  $(47.35–53.99) \times 10^{-3}$  SI units in andesites; and the  $k$ -value in the daciandesite sample is  $48.46 \times 10^{-3}$  SI units (Table 1).

The rock magnetic investigations were carried out for three samples dredged from the northeastern edifice (porphyric andesibasalts samples B17-51/2 and B17-51/4 and aphyric andesibasalts sample B17-51/8) and two samples from the southwestern edifice (porphyric daciandesite sample B40-26/2 and aphyric basalt sample B40-26/3) (Table 3). The magnetization of the porphyric species varies within 0.68–1.70 A/m and is by one order of magnitude lower than of the aphyric samples. In contrast, their magnetic susceptibility is double or triple as high as in the aphyric samples; it varies within  $(39.3–48.46) \times 10^{-3}$  SI units (Table 3). The aphyric varieties have NRM ranging within 10.18–31.56 A/m and  $k$ , within  $(16.29–19.23) \times 10^{-3}$  SI units (Table 3). The degree of  $P'$  in the samples varies from 1.012 to 1.056.

The magnetization of the porphyric varieties is caused by the extensive presence of large MD grains of low-coercive magnetic minerals. This is indicated by the values of  $B_{cr} = 17–18$  mT,  $B_{0.5} = 9–28$  mT, and ratios  $J_{rs}/J_s$ ,  $B_{cr}/B_c$  (Table 3). The magnetization of the aphyric varieties is due to the presence of PSD grains of the magnetic minerals with a higher coercive force ( $B_{cr} = 28–41$  mT) and a high median magnetic field ( $B_{0.5} \geq 100$  mT). The variations in the NRM values are accounted for by the differences in the domain structure of titanomagnetite caused by the different crystallization conditions of the basalt melt. In the marginal parts of the basalt flows, the melt rapidly cools, and aphyric basalts are formed. Under these conditions, the titanomagnetite crystals acquire the SD and PSD structure. These rocks have the highest NRM. Within the internal areas of the basalt flows, the crystallization progresses much more slowly, and the MD titanomagnetite crystals with the lower NRM are formed (Priroda ..., 1996).

The TMA from  $J_{rs}(T)$  for the porphyric andesite–basalt sample B17-51/4 has shown that the sample loses magnetization at ~540°C (Fig. 3). The TMA curve of the second heating goes above the curve of the first heating and follows its behavior. Its blocking temperature increases to ~560°C, which is close to the  $T_c$  of magnetite. Hence, the main magnetic mineral that carries the magnetization in this sample is titanomagnetite with low Ti-content  $X \sim 0.05$ . After heating,

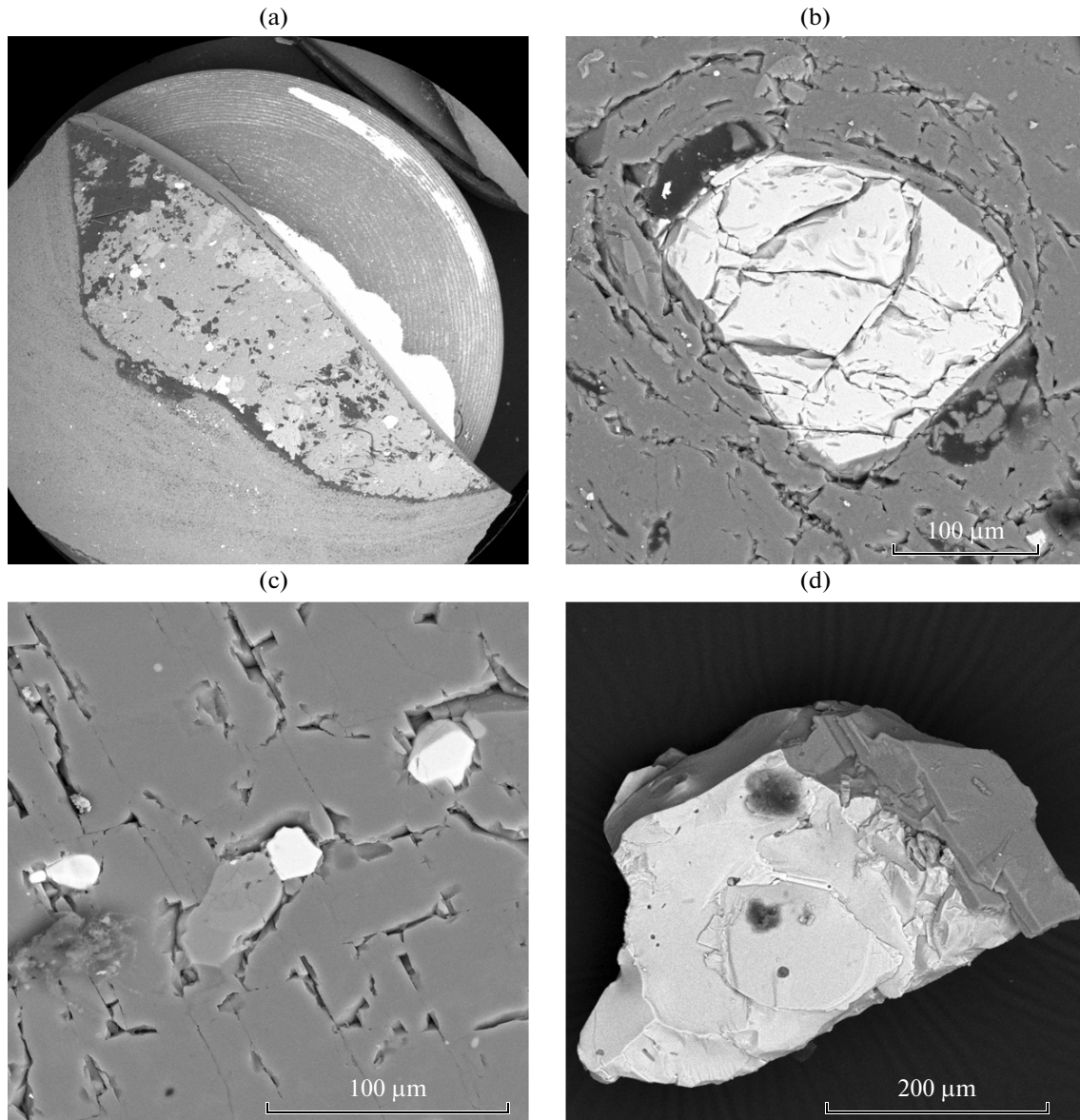


**Fig. 8.** Titanomagnetites from the Smirnov submarine volcano (sample B11-73/20): (a), the overall view of the thin section. The gas voids having different sizes as well as titanomagnetite phenocrysts and microlites (bright white spots and points in the interior part of the section, not to be confused with the white rim of the glue beyond the section area) are nonuniformly distributed across the thin section; (b), titanomagnetite phenocryst encircled by the groundmass; (c), titanomagnetite microlites enclosed in the pyroxene crystal; (d), the volumetric titanomagnetite crystal coated by the glassy groundmass jacket and containing the carbon-rich inclusions (organic matter, probably bitumen) (dark gray inclusions).

titanomagnetite undergoes heterophase disintegration with the formation of magnetite, which has a high remanent magnetization, and ilmenite.

The twin specimen of the porphyric andesibasalts sample B17-51/4 was subjected to TMA from  $J_s(T)$ , which has also demonstrated the high Curie point  $T_c \sim 480^\circ\text{C}$  in the curve of the first heating and its small displacement to  $490^\circ\text{C}$  in the cooling curve (Fig. 4). The heating and cooling curves are practically reversible and coincident. It can be assumed that oxidation of the primary titanomagnetite in this sample had already

occurred under the natural conditions (Pechersky and Didenko, 1995).

The petrographical investigations and microprobe analysis of the B17-51/4 sample show that it is porphyric olivine-pyroxene-amphibole-plagioclase andesibasalt with biotite, with the glassy ground mass saturated by the finest ore dust up to the opaque state (opacite groundmass). The phenocryst/groundmass ratio is 3/1 (Fig. 9).

The crystals of the ore mineral are scattered across the groundmass and form the intergrowths with oliv-

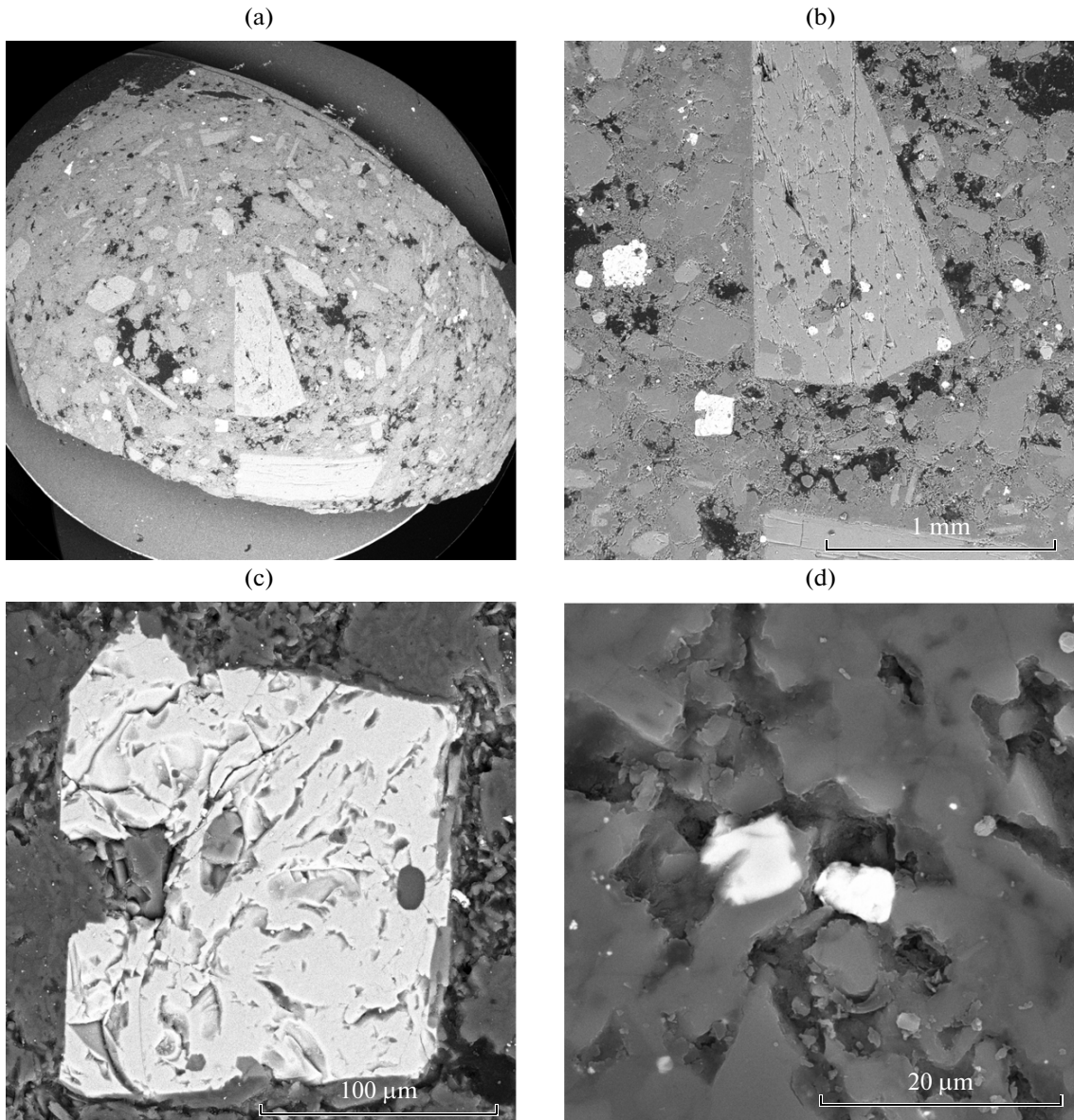


**Fig. 9.** Titanomagnetites from the Edelshtein submarine volcanic massif (sample B17-51/4): (a), the overall view of the thin section. Large amphibole inclusions and smaller pyroxene and ore material inclusions are present; (b), the area of the thin section with clearly seen titanomagnetite phenocryst and microlite precipitates (in particular, titanomagnetite inclusions within the amphibole crystal); (c), titanomagnetite phenocryst with apatite inclusions inside (gray and dark gray inclusions), uneven dislocated surface of the crystal is seen; (d), titanomagnetite microlites in the glassy groundmass.

ine, amphibole, and pyroxene. The crystal sizes are up to  $0.4 \times 0.4$  mm. Intergrowths of several titanomagnetite crystals are frequent. The groundmass contains finest titanomagnetite microlites ( $0.02 \times 0.02$  mm).

The chemical composition of the ore mineral from the Edelshtein volcano is presented in Table 4. The difference in the titanomagnetite compositions determined in the thin sections and in the selected grains is remarkable. In the first case, the number of all cations is significantly higher except for iron whose total content decreases by  $\sim 1\%$ . However, the mineral formula

recalculation from the compositions of mineral varieties indicates that this decrease mainly affects the  $\text{Fe}^{3+}$  cations. The Ti content remains approximately the same in both cases. Although the compositions of the different morphological varieties and the analyses on the surface and interior parts slightly differ, the mineral formulas are close. They are characterized by the substitution of trivalent Fe by Ti by  $X = 0.16$  and  $0.17$  f.u. per unit cell, which probably lies within the errors of recalculation and analysis.

**Table 5.** The relationship between Ti content per unit mineral cell and the Curie points for the submarine volcanoes on the Sea-of-Okhotsk slope in the northern part of KIA

Submarine volcano	Ti content per unit cell, f.u.	Curie point (°C)
Grigor'ev volcano	0.28–0.42	270–370
	0.14–0.24 inclusions in minerals	420–490
The 1.4 volcano	0.13–0.17	450–480
Belyankin volcano	0.23–0.29	410–470
Smirnov volcano	0.14–0.16	490–510
	Ore in xenoliths	700
Edelshtein volcano	0.16–0.18	470–510

The obtained titanomagnetite formula recalculated from the average (over 16 analyses) composition is  $(\text{Fe}_{0.86}^{+2}\text{Mg}_{0.06}\text{Mn}_{0.03})_{0.95}(\text{Fe}_{1.72}^{+3}\text{Ti}_{0.16}\text{Al}_{0.09}\text{V}_{0.01})_{1.99}\text{O}_{4.00}$ .

The average Ti content per unit mineral cell is determined at  $X = 0.16$  f.u.; the variations in the Ti content in the macro- and micrograins are  $X = 0.14$ – $0.18$  f.u. This corresponds to the Curie points in the interval  $T_c = 470$ – $510^\circ\text{C}$  which accommodates the range of the Curie points obtained in the TMA experiments with  $J_s(T)$ . Thus, the main magnetization carrier in this sample is titanomagnetite with a low Ti content.

## DISCUSSION

Our rock magnetic and microprobe studies have shown that the magnetization in the studied porphyric and aphyric varieties of the dacite-basalt rocks series is mainly carried by the PSD and MD grains of titanomagnetite and Ti-depleted titanomagnetite with minor admixtures of Mg, Al, V, and Mn. The high magnetization values are largely due to the PSD structure of the titanomagnetite grains, whereas the high values of the magnetic susceptibility are associated with the high concentration of the ferrimagnetic grains. The bulk concentration of ferrimagnetic in the volcanic rock samples,  $C$ , varies within  $\sim 0.6$ – $1.8\%$  (Table 3). In the calculations of the bulk concentration, we used the values of saturation magnetization of the samples estimated in the experiments from the magnetic hysteresis curves and the saturation magnetization of titanomagnetite determined from the atomic fraction of Ti (Butler, 1998). Among the studied samples, the ones containing PSD titanomagnetite grains are most magnetically stable; the samples with MD grains are less stable (Table 3, parameter  $Q_n$ ).

Across the studied samples, NRM tends to decrease with the growth of magnetic susceptibility,

which is probably due to the dependence of the magnetic characteristics on the grain size (Butler, 1998; Dunlop, 1981). The similar pattern of NRM behavior with the increase in magnetic susceptibility was also noted in the studies of basalts from the rift zone in the southern regions of the Red Sea (Trukhin et al., 2006).

The samples dredged from the Smirnov submarine volcano and some samples from volcanoes 1.4, Belyankin, and the Edelshtein massif have  $Q_n < 1$ , which may indicate that the interpretation of the magnetic anomalies  $\Delta T_a$  above these edifices should probably also take into account the contribution of the induced magnetization.

Although according to the present-day notions igneous rocks are close to isotropic (Pechersky and Didenko, 1995), it was established that some samples dragged from the Belyankin, Smirnov, and Edelshtein submarine volcanoes have slightly higher AMS values (Table 3), which indicates that the crystallization of the magnetic minerals occurred in the environment of the directed pressure and currents.

The microprobe analysis has not detected heterophase alteration of titanomagnetite and its exsolution structures in any studied samples, although the high Curie points and high values of the median magnetic field  $B_{0.5}$  in some samples point to the phase transformations and compositional changes of titanomagnetite. The measured  $T_c$  are frequently higher than the calculated ones and in many cases are close to  $T_c$  of magnetite. The formation of the hardly recognizable fine exsolution structures of this type was noted in (Pechersky and Didenko, 1995).

If we assume that the lower Ti content in titanomagnetite corresponds to the higher temperature of its formation, then the highest-temperature titanomagnetites are those from the Smirnov, Edelshtein, and 1.4 volcanoes (Table 5), which is directly related to the latest equilibrium state of the magma and to the depth of the magma chamber (Pechersky and Didenko, 1995). Titanomagnetites from the Belyankin and Grigor'ev volcanoes have a lower formation temperature.

The comparative analysis of the magnetic properties of the rocks composing the submarine volcanoes on the Sea-of-Okhotsk slope of the northern part of KIA shows that, just as in the Izu-Bonin, Mariana, and Solomon island arcs (Pilipenko and Rashidov, 2013; Pilipenko et al., 2012a; 2012b; 2014a; 2014b; Rashidov et al., 2012; 2014, 2015), the rocks are strongly differentiated in terms of NRM,  $k$ , and  $Q_n$  values. This differentiation is due to the presence of several ferrimagnetics, which were formed both during the crystallization of the rock and after its alteration as a result of secondary processes.

## CONCLUSIONS

Our studies complement the existing data on the magnetic properties, structural, and petrographical-mineralogical features of the rocks composing the edi-

fices of the submarine volcanoes in the western part of the Pacific transition zone, which could be treated in the future from various standpoints.

It is established that the rocks composing the submarine volcanoes on the Sea-of-Okhotsk slope in the northern part of KIA are strongly differentiated by the values of NRM,  $k$ , and  $Q_n$ . It is shown that the high NRM values in the studied rocks are due to the PSD structure of the titanomagnetite grains, whereas the high  $k$  are accounted for by the high concentration of the ferrimagnetic grains. The highest-temperature titanomagnetites are those from the Smirnov, Edelsh-tein, and 1.4 volcanoes.

The obtained data can be helpful in the interpretation of the anomalous magnetic field in the regions of island arc volcanism in the Pacific and in the studies on the acquisition of magnetic remanence by the rocks during the evolution of volcanic edifices.

#### ACKNOWLEDGMENTS

The work was supported by the Russian Foundation for Basic Research (project no. 15-05-02955-a).

#### REFERENCES

- Anikeeva, L.I., Kazakova, V.E., Gavrilenko, G.M., and Rashidov, V.A., Ferromanganese crust formations of the West Pacific transition zone, *Vestn. KRAUNTS. Nauki Zemle*, 2008, vol. 11, pp. 10–31.
- Babayants, P.S., Blokh, Yu.I., Bondarenko, V.I., Rashidov, V.A., and Trusov, A.A., Application of the Sigma-3D software package for structural interpretation of submarine volcanoes of the Kurile Island Arc, *Vestn. KRAUNTS. Nauki Zemle*, 2005, vol. 6, pp. 67–76.
- Babayants, P.S., Blokh, Yu.I., Bondarenko, V.I., Rashidov, V.A., and Trusov, A.A. 3D modeling of the submarine volcanoes of the Kuril Island Arc, *Voprosy teorii i praktiki geologicheskoi interpretatsii gravitatsionnykh magnitnykh i elektricheskikh polei: Materialy 33-ei sessii Mezhdunarodnogo seminar im. D.G. Uspenskogo* (Theory and Practice of Geological Interpretation of Gravity, Magnetic, and Electric Fields: Proc. 33rd Session of D.G. Uspenskii Int. Workshop), Ekaterinburg, January 30–February 3, 2006, Yekaterinburg: Inst. Geofiz. UrO RAN, 2006, pp.16–21.
- Bezrukov, P.L., Zenkevich, N.L., Kanaev, V.F., and Udintsev, G.B., Seamounts and submarine volcanoes of the Kuril Island Arc, in *Tr. Laboratorii Vulkanologii* (Proc. Laboratory of Volcanology), 1958, vol. 13, pp. 71–88.
- Blokh, Yu.I., Bondarenko, V.I., Rashidov, V.A., and Trusov, A.A., The Grigor'ev submarine volcano (Kuril island arc), *Vulkanol. Seismol.*, 2006a, no. 5, pp. 17–26.
- Blokh, Yu.I., Bondarenko, V.I., Rashidov, V.A., and Trusov, A.A., The Alaid volcanic massif (Kuril island arc), *Materialy mezhdunarodnogo simpoziuma "Problemy eksplozivnogo vulkanizma" k 50-letiyu katastroficheskogo izverzheniya vulkana Bezmyannyi* (Proc. Int. Symp. "Problems of Explosive Volcanism" Commemorating the 50th Anniversary of the Bezmyannyi Volcano Catastrophic Eruption), March 25–30, 2006, Petropavlovsk-Kamchatskii, Gordeev, E.I., Ed., Petropavlovsk-Kamchatskii: IViS DVO RAN, 2006b, pp. 135–143.
- Blokh, Yu.I., Bondarenko, V.I., Dolgal, A.S., Novikova, P.N., Rashidov, V.A., and Trusov, A.A., Modern techniques for interdisciplinary investigation of submarine volcano 6.1 in the Kurile island arc, *Geofizika*, 2012a, no. 2, pp. 58–66.
- Blokh, Yu.I., Bondarenko, V.I., Dolgal, A.S., Novikova, P.N., Rashidov, V.A., and Trusov, A.A., Modern techniques for interdisciplinary investigation of submarine Makarov volcano (the Kurile island arc), *Geoinformatika*, 2012b, no. 4, pp. 8–17.
- Blokh, V.I., Bondarenko, V.I., Dolgal, A.S., Novikova, P.N., Rashidov, V.A., and Trusov, A.A., Complex modeling of submarine volcanoes 2.7 and 2.8, the Kurile island arc, *Vestn. KRAUNTS, Nauki Zemle*, 2013a, vol. 21, pp. 77–85.
- Blokh, Yu.I., Bondarenko, V.I., Dolgal, A.S., Novikova, P.N., Rashidov, V.A., and Trusov, A.A., Combined geophysical studies of the Rikord massif (Kuril island arc), *Materialy regional'noi konferentsii. "Vulkanizm i svyazannye s nim professy". posvyashchennoi Dnyu vulkanologa, 29–30 marta 2013g.* (Proc. Regional Conf. "Volcanism and Related Processes" on the Occasion of Volcanologists Day, March 29–30, 2013) Gordeev, E.I., Ed., Petropavlovsk-Kamchatskii: IViS DVO RAN, 2013b, pp. 167–173.
- Blokh, Yu.I., Bondarenko, V.I., Dolgal, A.S., Novikova, P.N., Pilipenko, O.V., Rashidov, V.A., and Trusov, A.A., Application of modern computer technologies for investigation of submarine volcanic centre near the south-western coast of Simushir Island, the Kurile Island Arc, *Vestn. KRAUNTS, Nauki Zemle*, 2014a, no. 24, pp. 27–40.
- Blokh, Yu.I., Bondarenko, V.I., Dolgal, A.S., Novikova, P.N., Rashidov, V.A., and Trusov, A.A., Geophysical studies of the submarine volcanic center near the southwestern termination of the Simushir Island (Kuril Island Arc), *Voprosy teorii i praktiki geologicheskoi interpretatsii gravitatsionnykh magnitnykh i elektricheskikh polei: Materialy 41-oi sessii Mezhdunarodnogo seminar im. D.G. Uspenskogo* (Theory and Practice of Geological Interpretation of Gravity, Magnetic, and Electric Fields: Proc. 41st Session of D.G. Uspenskii Int. Workshop), Ekaterinburg, January 27–31, 2014, Yekaterinburg: Inst. Geofiz. UrO RAN, 2014b, pp.44–46.
- Bondarenko, V.I., Rashidov, V.A., Seliverstov, N.I., and Shkira, V.A., The submarine volcano west of the Paramushir Island, *Vulkanol. Seismol.*, 1994, no. 1, pp. 13–18.
- Brusilovskii, Yu.V., Ivanenko, A.N., and Rashidov, V.A., Analysis of magnetic fields above three Late Cenozoic submarine volcanoes, northern Kuril island arc, *Vulkanol. Seismol.*, 2004, no. 2, pp. 73–80.
- Butler, R., Paleomagnetism: magnetic domains to geologic terranes. Electronic edition, May 1998. Department of Geosciences, University of Arizona, Tucson, Arizona. <http://www.pmc.ucsc.edu/~njarboe/pmagresource/ButlerPaleomagnetismBook.pdf>
- Carvalho, C., Özdemir, Ö., and Dunlop, D.J., Palaeointensity determinations, palaeodirections and magnetic properties of basalts from the Emperor seamounts, *Gophys. J. Int.*, 2004, vol. 156, pp. 29–38.
- Day, R., Fuller, M., and Schmidt, V.A., Hysteresis properties of titanomagnetites: grain-size and compositional dependence, *Phys. Earth Planet. Inter.*, 1977, vol. 13, pp. 260–267.
- Didenko, A.N., The study of the compositions of titanomagnetites in the basalts of the Zelenyi Mys fault (Central

- Atlantic), *Dokl. Akad. Nauk SSSR*, 1989, vol. 309, no. 3, pp. 667–669.
- Didenko, A.N. and Tikhonov, L.V., Petro-magnetic investigation of basalts, in *Siroenie razloma Doldrams. Tsentral'naya Atlantika* (The Structure of the Doldrams Fault, Central Atlantic), Pushcharovskii, Yu.M., Ed., Moscow: Nauka, 1991, pp. 112–131.
- Didenko, A.N., Peive, A.A., and Tikhonov, L.V., Petro-magnetic and petrological variations along the Mid-Atlantic and Southwestern Indian Ridges in the Bouvet Triple Junction region, *Izv. Phys. Solid Earth*, 1999, vol. 35, no. 12, pp. 1010–1027.
- Dunlop, D.J., The rock magnetism of fine particles, *Phys. Earth Planet. Int.*, 1981, vol. 26, pp. 1–26.
- Ermakov, V.A. and Pecherskii, D.M., The nature of gabbroid inclusions from the young lavas of the Kurile islands, *Tikhookean. Geol.*, 1989, no. 4, pp. 45–55.
- Evans, M.E. and Heller, F., *Environmental Magnetism: Principles and Applications of Enviromagnetics*, Amsterdam: Academic, 2003.
- Geologo-geofizicheskii atlas Kurilo-Kamchatskoi ostrovnoi sistemy* (Geological-Geophysical Atlas of the Kuril–Kamchatka Island System), Sergeev, K.S. and Krasnii, M.L., Eds., Leningrad: VSEGEI, 1987.
- Kichina, E.N. and Ostapenko, V.F., Alkali basalts of the Belyankin submarine volcano (Sea of Okhotsk), *Dokl. Akad. Nauk SSSR*, 1977, vol. 232, no. 1, pp. 205–208.
- Kochergin, E.V., Pavlov, Yu.A., and Sergeev, K.F., *Geomagnitnye anomalii Kuril'skoi i Ryukyu ostrovnykh sistem* (Geomagnetic Anomalies of the Kuril and Ryukyu Island Systems), Moscow: Nauka, 1980.
- Kontny, A., Vähle, C., and de Wall, H., Characteristic magnetic behavior of subaerial and submarine lava units from the Hawaiian Scientific Drilling Project (HSDP-2), *Geochem. Geophys. Geosyst.*, 2003, vol. 4, no. 2, p. 31. doi 10.1029/2002GC000304
- Korenev, O.S. and Shkut', G.I., On the magnetic susceptibility of the rocks in the northern part of the Kuril arc, in *Geofizicheskie polya ostrovnykh dug Vostoka Azii* (Geophysical Fields of Island Arcs in the East Asia), Vladivostok: DVNTs AN SSSR, 1979, pp. 45–50.
- Korenev, O.S., Neverov, Yu.L., Ostapenko, V.F., Zhigulev, V.V., Kichina, E.N., Krasnyi, M.L., and Khomyakov, V.D., The results of geological dredging in the Sea of Okhotsk from aboard the Pegas research vessel (21st cruise), in *Geologicheskoe stroenie Okhotomorskogo regiona* (Geological Structure of the Sea of Okhotsk Region), Vladivostok: SakhKNII DVNTs AN SSSR, 1982, pp. 36–51.
- Korenev, O.S., Geomagnetic formations in the basement of the Okhotsk Basin, *Tikhookean. Geol.*, 1990, no. 2, pp. 33–41.
- Kurochkina, E.S., Magnetic properties of submarine basalts and the evolution of the Red Sea rift zone, *Extended Abstract of Cand. Sci. (Phys.-Math.) Dissertation*, Moscow: Moscow State University, 2007.
- Magnitnoe pole okeana* (Magnetic Field of the Ocean) Gordnitskii, A.M., Ed., Moscow: Nauka, 1993.
- Ostapenko, V.F., Some aspects of the recent evolution of the near-Kuril part of the Sea of Okhotsk in the light of studying of the submarine volcanoes in this region, in *Vulkanizm Kurilo-Kamchatskogo regiona i o. Sakhalin* (Volcanism of the Kuril–Kamchatka Region and Sakhalin Island), Yuzhno-Sakhalinsk: DVNTs AN SSSR, 1976, pp. 34–74.
- Ostapenko, V.F. and Kichina, E.N., Material composition of the lavas from submarine volcanoes of the Kuril arc, in *Geologiya dna Dal'nevostochnykh morei* (Sea Floor Geology of the Far Eastern Seas), Vladivostok: DVNTs AN SSSR, 1977, pp. 24–45.
- Ostapenko, V.F., Submarine volcanoes in the near-Kuril part of the Sea of Okhotsk and their value for understanding the recent evolution of this region, *Dokl. Akad. Nauk SSSR*, 1978, vol. 242, no. 1, pp. 168–171.
- Ostapenko, V.F. and Kichina, E.N., Lateral variations in the petrographic composition of the lavas from the surface and submarine volcanoes of the Great Kuril Arc, in *Rel'ef i vulkanizm Kuril'skoi ostrovoduzhnoi sistemy* (Topography and Volcanism of the Kuril Island Arc System), Vladivostok: DVNTs AN SSSR, 1982, pp. 74–90.
- Pecherskii, D.M., Zolotarev, B.P., and Tikhonov, L.V., Magmatism of the Atlantic basalts, *Izv. Akad. Nauk SSSR, Fiz. Zemli*, 1979, no. 12, pp. 67–84.
- Pecherskii, D.M., Lykov, A.V., Tikhonov, L.V., and Sharas'kin, A.Ya., Magnetic properties of igneous rocks in the region of Philippines Sea and Mariana Trench, in *Reshenie geofizicheskikh zadach geomagnitnymi metodami* (Solving the Geophysical Problems by Magnetic Methods), Moscow: IFZ AN SSSR, 1980.
- Pecherskii, D.M., Tikhonov, L.V., and Zolotarev, B.P., Magnetism and paleomagnetism of basalts in the Gulf of California, *Izv. Akad. Nauk SSSR, Fiz. Zemli*, 1981, no. 9, pp. 51–64.
- Pecherskii, D.M. and Didenko, A.N., *Paleoaziatskii okean; petromagnitnaya i paleomagnitnaya informatsiya o ego litosfere* (Paleo-Asian Ocean; Rock Magnetic and Paleomagnetic Information about Its Lithosphere), Moscow: OIFZ RAN, 1995.
- Pilipenko, O.V., Rashidov, V.A., and Ladygin, V.M., Magnetic studies of the rocks from the Late Cenozoic submarine volcanoes in the island arcs of western Pacific, *Materialy II Shkoly - seminara "Gordinskie chteniya"* (Proc. 2nd Workshop "Gordin's Readings"), Moscow, November 21–23, 2012, Moscow: IFZ RAN, 2012a, pp. 160–164.
- Pilipenko, O.V., Rashidov, V.A., and Ladygin, V.M., Magnetic and petrophysical studies of the rocks of Late Cenozoic submarine volcanoes of western Pacific, *Paleomagnetizm i magnetizm gornykh porod. Materialy mezhdunarodnoi shkoly-seminara po problemam paleomagnetizma i magnetizma gornykh porod* (Paleomagnetism and Rock Magnetism. Proc. Int. Workshop on the Problems of Paleomagnetism and Rock Magnetism), St. Petersburg: SOLO, 2012b, pp. 184–191.
- Pilipenko, O.V. and Rashidov, V.A., Magnetic studies of the rocks of submarine volcanoes of the Izu-Bonin and Kuril island arcs, *Geologiya morei i okeanov. Materialy XX Mezhdunarodnoi nauchnoi konferentsii (Shkoly) po morskoi geologii* (Geology of Seas and Oceans. Proc. 20th Int. Workshop on Marine Geology), Moscow, November 18–22, 2013, Moscow: GEOS, 2013, vol. 5, pp. 209–213.
- Pilipenko, O.V., Rashidov, V.A., and Petrova, V.V., Magnetic studies of the rocks of submarine volcanoes of the Kuril island arc, *Paleomagnetizm i magnetizm gornykh porod. Materialy mezhdunarodnoi shkoly-seminara po problemam paleomagnetizma i magnetizma gornykh porod* (Paleomagnetism and Rock Magnetism. Proc. Int. Workshop on the Problems of Paleomagnetism and Rock Magnetism), St. Petersburg: SOLO, 2014a, pp. 131–140.

- Pilipenko, O.V., Rashidov, V.A., and Petrova, V.V., Petro-magnetism of igneous rocks of the submarine volcanoes from Kurile Island Arc, *10th Int. Conf. "Problems of Geocosmos," Book of Abstracts*, St. Petersburg, Petrodvorets, Oct. 6–10, 2014, St.-Petersburg: Russian Foundation of Basic Research, 2014b, pp. 66–67.
- Plate Tectonics*, Le Pichon, X., Francheteau, J. and Bonnin, J., Eds, Amsterdam: Elsevier, 1973.
- Podvodnyi vulkanizm i zonal'nost' Kuril'skoi ostrovnnoi dugi* (Submarine Volcanism and Zonality of the Kuril Island Arc), Pushcharovskii, Yu.M., Ed., Moscow: Nauka, 1992.
- Popov, K.V., Shcherbakov, V.P., Gorodnitskii, A.M., and Nazarova, E.A., Magnetic characteristics of the oceanic crustal rocks in the zone of the Clarion transform fault, *Byull. Mosk. O-va. Ispyt. Prir., Otd. Geol.*, 1989, vol. 6, no. 3, pp. 34–44.
- Popov, K.V. and Shcherbakov, V.P., Magnetic properties of the ferrobasalts of the Shatsky Rise, the Pacific Ocean, *Oceanology*, 2001, vol. 41, no. 4, pp. 545–553.
- Popov, K.V., Bazylev, B.A., Shcherbakov, V.P., and Gapeev, A.K., Comparison between the magnetic and petrological characteristics of the peridotites from the Goringe Ridge and the peridotites from the mid-ocean ridges, *Oceanology*, 2011, vol. 51, no. 1, pp. 157–169.
- Priroda magnitnykh anomalii i stroenie okeanicheskoi kory* (The Nature of Magnetic Anomalies and the Structure of the Oceanic Crust), Gorodnitskii, A.M., Eds., Moscow: VNIRO, 1996.
- Rashidov, V.A., Sazonov, A.P., Seliverstov, N.I., and Shkira, V.A., New data on the manifestation of submarine volcanism west of the Paramushir island, in *Vulkanizm, struktury i rudobrazovanie: Tez. dokl. 7 Vses. Vulkanologicheskogo soveshchaniya* (Volcanism, Structures and Ore Formation. Abstracts 7th All-Russia Volcanology Conference), Petropavlovsk-Kamchatskii, 1992, pp. 64–65.
- Rashidov, V.A. and Bondarenko, V.I., Geophysical studies of the Belyankin and Smirnov submarine volcanoes (Kuril island arc), *Vulkanol. Seismol.*, 1998, no. 6, pp. 107–114.
- Rashidov, V.A. and Bondarenko, V.I., The Edelstein submarine volcanic massif (Kuril island arc), *Vulkanol. Seismol.*, 2003, no. 1, pp. 3–13.
- Rashidov, V.A. and Bondarenko, V.I., Geophysical studies of the Krylatka submarine volcano (Kuril island arc), *Vulkanol. Seismol.*, 2004, no. 4, pp. 65–76.
- Rashidov, V.A., Geomagnetic investigations at the studies of submarine volcanoes in the island arcs and marginal seas of the West Pacific, *Extended Abstract of Cand. Sci. (Tech.) Dissertation*, Schmidt Institute of Physics of the Earth of the Russian Academy of Sciences, Moscow, 2010.
- Rashidov, V.A., Pilipenko, O.V., and Ladygin, V.M., Petro-magnetic investigations of active submarine volcanoes from western Pacific Ocean, *9th Int. Conf. "Problems of Geocosmos," Book of Abstracts*, St. Petersburg, Petrodvorets, Oct. 8–12, 2012, St. Petersburg, 2012, pp. 68–69.
- Rashidov, V.A., Pilipenko, O.V., and Ladygin, V.M., A comparative analysis of magnetic properties in rocks: five active submarine volcanoes in the Western Pacific, *J. Volcanol. Seismol.*, 2014, vol. 8, no. 3, pp. 168–182.
- Rashidov, V.A., Pilipenko, O.V., and Petrova, V.V., Petro-magnetic and microprobe studies of rocks in the Sofu underwater volcanic cluster, Izu–Bonin island arc, Pacific Ocean, *J. Volcanol. Seismol.*, 2015, vol. 9, no. 3, pp. 182–196.
- Shreider, A.A., Rimskii-Korsakov, N.A., and Trukhin, V.I., The detailed geomagnetic studies of the rift zone in the south of the Red Sea, *Okeanologiya*, 1982, vol. 22, no. 3, pp. 439–445.
- Stokking, L.B., Merrill, D.L., Haston, R.B., Ali, J.R., and Saboda, K.L., Rock magnetic studies of serpentinite seamounts in the Mariana and Izu–Bonin regions, *Proc. Ocean Drilling Program, Scientific Results*, 1992, vol. 125, pp. 561–579.
- Trukhin, V.I., Bagin, V.I., Bulychev, A.A., Gilod, D.A., Zhilyaeva, V.A., Tomilin, E.F., Shreider, A.A., and Shubin, I.A., Magnetism of the Spiess mid-ocean ridge, South Atlantic, *Izv., Phys. Solid Earth*, 2000, vol. 36, no. 2, pp. 161–174.
- Trukhin, V.I., Shreider, A.A., Bagin, V.I., Bulychev, A.A., Gilod, D.A., Zhilyaeva, V.A., and Aleksandrov, D.V., The sea-floor magnetism in the Bouvet transform zone, south Atlantic, *Izv., Phys. Solid Earth*, 2001, vol. 37, no. 6, pp. 517–525.
- Trukhin, V.I., Shreider, A.A., Zhilyaeva, V.A., Bulychev, A.A., and Maksimochkin, V.I., Seafloor magnetism in the Romanche transform zone (the equatorial Atlantic), *Izv., Phys. Solid Earth*, 2005, vol. 41, no. 3, pp. 179–192.
- Trukhin, V.I., Maksimochkin, V.I., Zhilyaeva, V.A., Kurochkina, E.S., Shreider, A.A., and Kashintsev, G.L., Magnetic properties of basalts and geodynamics of the rift zone in the southern Red Sea, *Izv., Phys. Solid Earth*, 2006, vol. 42, no. 11, pp. 928–941.
- Verba, V.I., Avetisov, G.P., Sholpo, L. Ye., and Stepanova, T.V., Basalts geodynamikes and magnetism of the Knipovich underwater ridge (Norway–Greenland basin), *Ros. Zh. Nauk Zemle*, 2000, vol. 2, no. 3, pp. 303–312.

*Translated by M. Nazarenko*